

Physicochemical characterisation of bio-based insulation to explain their hygrothermal behaviour

Abbie Romano¹, Sotirios Grammatikos², Mike Riley¹ and Ana Bras¹

¹Built Environment and Sustainable Technologies (BEST) Research Institute, Department of Built Environment, Liverpool John Moores University, Byrom Street, Liverpool L3 3AF, UK

²Department of Manufacturing and Civil Engineering, Norwegian University of Science and Technology, 2815 Gjøvik, Norway

Abstract

The utilisation of bio-based building materials as hygric buffers has received recent research interest due to their moisture sorption and thermal behaviours which are positive for indoor comfort. Their hygrothermal properties are known but not fully understood, especially when these bio-based materials are exposed to frequent indoor relative humidity (RH) levels. For the first time, it is identified the characteristics at a micro-level responsible for the hygrothermal performance. Bio-based samples utilised within this paper are : Saw Mill Residue (SMR), Wool 1 (W1), Wool 2(W2), Wood Pellets (WP), Straw (STW) and Wood Wool Board (WWB). Results included thermal analysis (DSC, TGA, DTG), chemical analysis (FTIR) and optical microscopy (SEM) to understand and compare how these bio-based materials behave when stabilised at 53% and 75% RH. For cellulose based samples it was demonstrated that in a dynamic hygrothermal environment SMR and WP are the most hygrothermal stable and for keratin-based materials, W1 is the most stable. For the keratin-based samples when conditioned at 75%, as per the intensity of FTIR spectra, the regularity of molecular chain, W2 has the more ordered material structure but W1 is affected more in terms of hydroxyl absorbance from the spectra. These experiments give a greater insight into the dynamic way in which RH affects the thermal stability of samples. This research paper outlines fundamental differences within materials physical properties and chemical reactions. From the 6 different materials that were used, SMR was demonstrated to be the most thermally stable sample overall.

Keywords: hygrothermal, bio-based materials, TGA, DSC, FTIR, physicochemical

1. Introduction

1.1 General Introduction

The use of 'green energy' by countries intends to lower fossil fuel emissions and the overall global warming effect. To do so, protocols, regulations and the growing demand for the utilisation of bio-based building materials has never been greater [1] [2]. Continued urbanisation and the utilisation of fossil fuels has not only contributed to global warming but also reduced overall air quality [3]. Bio-based building materials contribute to the Energy/unrealised energy efficiency potential and has clear environmental and economic benefits [4]. This is highlighted by their considerably lower carbon emissions and improved storage by comparison to other 'conventional' building materials such as concrete or steel. Due to lack of current EU

regulation there are no governmental incentives for these materials and therefore their benefits are not realised, nor utilised.

As a fundamental basis, all materials are affected by parameters such as temperature and relative humidity [5]. High performing hygrothermal material are able to 'self-regulate' and buffer relative humidity. Bio-based insulation materials have hygrothermal characteristics which make them ideal for indoor relative humidity buffering. Insulation materials respond to seasonal adjustments in temperature in relative humidity due to their specific thermophysical properties. As effective insulator materials, they must have thermal comfort of the occupants at the centre of their characteristics – to be cooling in the summer and reduce heat requirements within the winter. The heterogeneous nature of bio-based and evolving climatic conditions ensure that a 'one size fits all' approach is insufficient in order to maximise the intrinsically beneficial hygrothermal characteristics[6].

Further fundamental benefits of bio-based building materials include their whole life considerations as they can be recycled (due to their biodegradability) and comparatively lower embodied energy and carbon to fossil fuel derived insulation products (such as polystyrene or polyurethane)[7] , which furthers the contribution of these construction materials for a 'closed production cycle' where waste is eradicated [8].The thermal degradation of bio-based materials has been explored by different researchers regarding individual bio-based materials but there is very limited literature using a combination of these materials[9, 10] .

The term 'hygrothermal' refers to the movement of heat and moisture through a materials or a group of materials. Temperature changes cause alterations in the physical and chemical properties of bio-based materials, which reflects on their hygrothermal behaviour and influence the overall properties of the final product. Moisture buffering capacity indicates the amount of water that is transported in or out of a material per open surface area, during a certain period of time, when it is subjected to variations in relative humidity of the surrounding air. A better understanding of the influence of temperature via the thermal analysis on the properties of bio-based materials enables to understand the behaviour and optimise the material. Due to the potential use of these materials in thermal energy storage or thermoregulation, an evaluation of thermal performance is important as thermal and hygrothermal parameters. Both of these characteristics depend on the temperature and moisture content of a material [5] . By exploring the relationship between relative humidity and biochemical reactions within bio-based materials it can be shown how these materials fundamentally differentiate. Despite this, the drawbacks of using these materials are the inhomogeneity due to external factors that the bio-based materials may experience such as seasonal variations, location/climate, soil conditions, etc.

As previously mentioned, bio-based insulation samples tend to be hygroscopic and therefore the moisture content greatly affects the materials thermal conductivity (as explored in [11] [12] and [5]. Investigations into the characteristics of bio-based materials (such as wool) at daily, household temperatures was explored in [13] and offers an insight into when water becomes trapped within the wool it limits the materials ability to act as an insulator in its entirety. This is due to water having a

much greater thermal conductivity value than that of air, so when materials are saturated in comparison to their dry state acts as a poor insulator – as explained in [14]. The effect of moisture having a linear relationship with thermal conductivity is also explained in [15] where wood and wood-based materials are characterised as the effects of moisture content on thermal conductivity value of wood-based fibre boards. This bio-based building material macro scale phenomenon of hygrothermal behaviour is explained at a molecular level, due to hydrogen bonding sites and methods of diffusion of water inside the material.

1.2. Hydroxyl Groups / Moisture Mechanisms

The fundamental mechanisms and hygrothermal ability of these materials are often attributed 'free' hydroxyl groups within the literature [16]. On a molecular level, water molecules consist of at least 2 hydrogen atoms and one oxygen which are polar and affects material properties as it is has a spatially-unbalanced distribution of charge – ensuring it is permanently polarised (which is visually represented in Figure 1). By comparison, hydroxyl groups are a functional group that consist of a hydrogen atom covalently bonded to an oxygen atom (denoted with -OH). As a highly reactive group, it quickly interacts with other molecules and the literature suggests that these groups provide a site for the hydrogen bonding on the surface of natural materials. This mechanism and 'likelihood' of hydroxyl groups to interact within these bio-based materials forms the basis of their theoretical hygrothermal background [17].

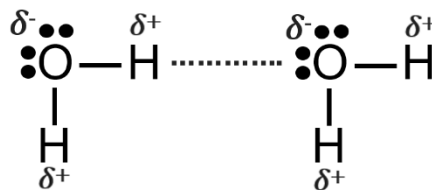


Figure 1. Polarised nature of water molecule.

The fundamental knowledge behind the hydroxyl group within a bio-based insulation material is incredibly important to understand the hygrothermal characteristics of these materials. These mechanisms and methods for the diffusion of water and way in which it moves through samples is important to understand as this will contribute to the hygrothermal performance of the material. Currently, there are several theories surrounding the adsorption of water into materials such as Brunauer-Emmett-Teller (BET) theory [18] as explained in [19] and Ficks law of diffusion and equilibrium, on the assumption of a uniaxial direction [20].

The complexities and issues surrounding these theories are that they apply a 'blanket' mechanisms for hygric materials and do not account for a constantly varying hygrothermal environment over a sustained period of time. Hydroxyl groups activities seem to be related to the hygrothermal behaviour of bio-based materials. However, the chemical and physical mechanisms behind this macro behaviour are not explicitly outlined by the scientific community which emphasise the need for answers.

1.3 Thermal Methods

Thermal methods enable to analyse the properties of materials as they change with temperature. Different methods can be used and they are distinguished from one another by the property which is measured (Figure 2).

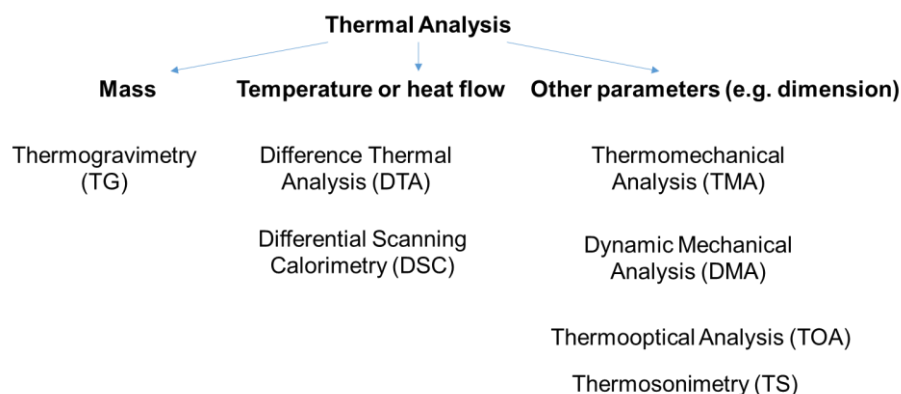


Figure 2. Parameter and methods of thermal analysis (based on [21]).

A key benefit of using thermal methods is that they provide quick and reliable results for the characteristics of materials. These include dehydroxylation which can be identified and denotes whereby heating a hydroxyl group is released and therefore a water molecule is formed [22]. However a drawback of this method is that as there is such a natural variability of different bio-based materials, different thermal conditions in which they are experimented will give differing results [23]. Due to its repeatability, thermal analysis is utilised as a method of characterising heterogeneous organic materials [24].

For Differential Scanning Calorimetry (DSC) measure the heat flow changes versus temperature or time. From the thermograms that are produced, endothermic reactions demonstrate information from the samples melting and transitioning in their phases, pyrolysis and evaporation whilst exothermic reactions give information on crystallisation, combustion, chemical reactions and decomposition [25]. DSC thermograms consider the peak of an endothermic reaction as the melting point. Peaks whose area corresponds to the enthalpy involved within the process – the shape of this peak demonstrates if the phase change is exothermic or endothermic. A change in heat flow within a sample demonstrates a change in the heat capacity of the sample. In order to understand that a thermal effect has taken place, this manifests as a deviation from an approximate straight line

Fourier Transform Infrared Spectroscopy (FTIR) spectroscopy aids the determination of chemical structure and can be generally split into two core sections: functional region and fingerprint region. For the functional region, its range is approximately $4000 - 1450 \text{ cm}^{-1}$ whereas the fingerprint region is from $1450 - 600 \text{ cm}^{-1}$. Thermo Gravimetric Analysis (TGA) measure mass change versus temperature or time. TGA combined with FTIR spectrometry is a hyphenated thermal analytical technique where volatiles released from a thermobalance are transferred through a heated transfer line to a heated cell inside a FTIR spectrometer acting as detector. Performing thermal analysis such as Thermogravimetric Analysis (TGA) and derivative thermogravimetry (DTG) on these bio-based materials enables to develop

the understanding for the way the reactions within the materials take place as a function of temperature and determines the thermal decomposition kinetic parameters.

Temperature changes cause alterations in the physical and chemical properties of bio-based materials, which can reflect on their hygrothermal behaviour and influence the overall properties of the final product. Chemical reactions such as hydrolysis, oxidation or reduction may be promoted, or physical changes, such as evaporation, melting, crystallization, condensation, etc may occur. A better understanding of the influence of temperature on the properties of bio-based materials enables to optimise processing conditions and tailor the product quality. It is therefore important for scientists to have analytical techniques to monitor the changes that occur in bio-based materials when their temperature varies. These techniques are often grouped under the general heading of thermal analysis.

2. Bio-fibre materials characteristics

Within this research paper, 6 different bio-based insulation materials were used: Saw Mill Residue (SMR), Wool 1 (W1), Wool 2(W2), Wood Pellets (WP), Straw (STW) and Wood Wool Board (WWB). Due to their fundamental differences, these materials can be further categorised into 2 key groups: cellulosic and keratin based samples.

2.1 Cellulose Based

The 'wood based' materials are manufactured from waste wood and these are utilised within these insulation materials as it comes from a variety of sources such as residual wood from industrial processes but also recycled wood[26]. On a cellular level, the key chemical components of wood based materials rely on cellulose as the main strength element within the material, hemicellulose binds monocrystalline hydrophilic cellulose with amorphous hydrophobic lignin. Lignin is hydrophobic and its role within the material is for structural support the materials whilst the carbohydrate (namely, cellulose) is hydrophilic. Formed by covalent bonds, cellulose maintains rigidity by transferring stress in order to reduce tensile stress and the formation of hydrogen bonds [27]. The structure of the cellulose within the material has a large and complex influence on the chemical reactions of this natural polymer.

Naturally a complex material, wood is considered a 'natural composite' consisting of lignin and carbohydrates but due to species variation there is an element of anatomical heterogeneity [28]. Lignin is a one of the most naturally abundant polymers and is located in the cell walls. By utilising thermal methods, heat flow is applied to wood-based materials and pyrolysis products are produced which affects the thermal production. As an inherently diverse natural insulation material, wood is a heterogeneous and anisotropic cellular material which depends on variations within both species and interspecies dependant [29]. In addition the location of the wood sample from within the tree (for example branch, trunk or roots etc.) will give differing material properties [30].

Understanding the molecular structure of a material is crucial to optimise its behaviour. Aside from identifying the functional groups bond behaviour, a key benefit of utilising Fourier Transform Infrared Spectroscopy (FTIR) for cellulose based materials is that the transmittance can indicate Total Crystallinity (TCI), Intensity of Hydrogen Bonding (HBI) and Lateral Order Index (LOI)[31]. TCI is calculated as the infrared crystallinity rate from [32] comparing absorption bands at C-H cellulose at 1370cm^{-1} and C-H bond of cellulose at CH_2 groups at 2900cm^{-1} . HBI considers the crystallinity of the molecule by examining the flexibility of the cellulose chains and the intensity of the hydrogen bonds within a sample [33] by comparing the absorption bands at 3400 cm^{-1} and 1320 cm^{-1} . Finally, LOI determines the way in which the crystal lattice can vary within the crystal lattice [33, 34] within crystalline zone at 1430cm^{-1} band and amorphous zone at 898cm^{-1} band. [35] suggests that the thermal stability of samples which are cellulose based are affected by the order of the crystalline. Therefore, the greater the LOI the more thermally stable the sample is.

Outlined in the literature, wood is affected by high relative humidity as its hygrothermal and capillary characteristics are affected within increased environmental water vapour and takes this moisture into the cell wall and cavities of the wood. In turn, this affects the dimensional stability of utilising these materials in construction[36] but actually boosts their utilisation as a hygrothermal buffer.

2.2 Keratin Based

Wool consists of many different amino acids which are linked together by peptide bonds to form polypeptides. Within the wool formation, keratin is formed of an α -crystal and β crystal. From the keratin molecules, these amino acids are formed from the core elements of Carbon, Hydrogen and Oxygen, the fibres chemical composition are keratin proteins which contain Nitrogen, Sulphur, Ash (comprising of calcium, phosphorus and sodium) [37]. Wool is an inherently complicated bio-based material due to its amorphous hygroscopic properties and as there is a polarity within the peptide groups of the macromolecule, salt linkages within the polymer [38-40]. Due to intrinsically natural variations, wool insulation within this research is comprised of several different breeds of sheep and equally a variation in diet and age. As a consequence, the amino acid and proteins within the wool will be heterogeneous.

Under normal atmospheric conditions wool contains around 15wt % absorbed moisture content. This relatively high moisture content within the material is a key consideration when investigating the hygrothermal conditions of these materials as this residual moisture may affect the material utilised in further experiments. Whilst the exterior of the material is hydrophobic, the interior is hygroscopic ensuring that the exchange of water can flow in and out of the sample but repels liquid water from the surface[41]. As outlined in [42] bio-based materials in hygrothermal environments are considered as a dynamic 3 phase system where there is the solid (sample matrix), liquid where the water vapour adsorbs to the surface of the samples (and therefore travels through the sample as liquid free water) and gas where the water vapour and air within the samples pores are. These materials ability to act as a hygric buffer is due to the continual equilibrium between these three dynamic states experience and their environment.

When the local hygrothermal and RH of the environment for which wool is in changes, the fibres exhibit a change in temperature, as the water vapour is adsorbed into the wools fibres it condenses and latent heat of sorption is produced as explored in [12]. Even as a bio-based material, wool is naturally flame resistant due to its protein structure and chemical composition associated with high content of nitrogen and sulphur [43] and when set alight is easily extinguished as it generally burns slowly [44] – demonstrating this materials natural flame retardant nature [45].

As a key characteristic of both cellulose and keratin based materials is their ability to optimally perform under differing hygrothermal conditions. Which includes not only the adsorption but also the desorption of water vapour within the material. This transition and transport of water molecular is of particular interest within this paper to see if this has further implications on the long term chemical structure of the sample. The use of bio-based materials has been investigated reviews on bio-based building materials such as [46] and [47] have no considered the physiochemical effect of different relative humidity's has. This paper will explore the thermal, chemical and physico properties of bio-based insulation materials at different relative humidity conditions.

3. Methods

3.1 Stabilisation of Samples

After being initially dried to BS EN ISO 12570, [48] each sample was conditioned and stabilised within a climatic chamber for 24 hours prior to testing. The hygrothermal conditions of 53% and 75% were selected as they are utilised in [49] and reflect the results of full-scale laboratory environmental conditions testing of a residential property.

3.2 Thermogravimetry Analysis (TGA) and derivative thermogravimetry (DTG)

As a quantitative technique thermogravimetric analysis (TGA) measures the mass change in a substance, as a function of temperature. As volatile compounds are lost, mass loss is demonstrated where the shape appears sigmoid in nature and graphically as a 'step'. By being able to utilise this type of thermal analysis it enables a deeper understanding of the thermal stability of the bio-based insulation materials.

For this research paper a TA Instruments, TGA Q50 was used, where samples were under scan conditions of 25 to 300°C at a linear rate of 20°C min⁻¹ under a Nitrogen atmosphere, using a circular, platinum crucible.

3.3 Differential Scanning Calorimetry (DSC)

As another quantitative method of thermal analysis, DSC measures heat flow rate, Q (W/g) differences from the samples being tested to an inert reference material as a function of the temperature and time taken. A Perkin Elmer DSC 7 was utilised with a temperature range of 25 to 300°C and heating conditions of 20°C/min in an oxygen free, nitrogen environment.

3.4 Fourier Transform Infrared Spectroscopy (FTIR)

This method of analysis utilises a wide spectral range simultaneously to collect an infrared spectrum, where each spectra demonstrates the functional groups according to the peak positions for every sample. Using an Agilent Technologies Cary 630 FTIR with a diamond crystal, which each spectra averaged over 128 scans over a 4000-650 cm^{-1} range.

3.5 Scanning Electron Microscopy (SEM)

To understand the surface morphology of the bio-based materials, SEM was utilised. This was performed on a Quanta Inspect S device. The accelerating voltage of the device was 20 kV, with a filament voltage of 2.0 – 2.3, Emission Current (EC) of ~100 and a set auto-bias to an EC of 100. Before testing, samples had a sputter coating in gold in order to prevent any charging of electrons to the sample.

4. Results and Discussion

4.1 TGA and DTG

For the purpose of these insulation materials to act as a hygric buffer of it is important to understand the reaction mechanism to heat them and how effectively bound water molecules evaporate. For each sample results, the TGA and DTG will be presented (where DTG is the first derivative of TGA).

This is important to understand in addition to their hygrothermal performance to give a more comprehensive understanding of these materials rather than just at laboratory conditions. Factors affecting the maximum decomposition rate and the location of the TGA curve are the heating rate. Therefore, similar conditions to other works have been selected in order align with them.

The TGA/DTG data for all samples can be found in Figures 3a to 3l. The objective of this analysis is to understand the thermal stability of the samples at different hygrothermal conditions (53% and 75% RH) so by examining this at the specific temperatures within Table 1 will give an adequate comparison of the materials behaviour. Comparing the performance of the samples at different temperatures demonstrates the nature of the materials crystallinity. Due to the clear variation in mass loss between the samples, a comparison between temperatures of 100°C and 300°C are shown in Table 1, for 53% and 75% RH for cellulose and Keratin based materials Bio-based samples utilised within this paper are that of: Saw Mill Residue (SMR), Straw (STW), Wood Pellets (WP), Wool 1 (WL1) and Wool 2 (WL2).

Table 1. Weight loss of all samples at 100°C and 300°C.

Sample	Weight loss % @ 100°C		Weight loss % @ 300°C	
	53% RH	75% RH	53% RH	75% RH
SMR	7.129	5.155	34.112	34.699
STW	4.403	8.846	32.731	26.176
WP	6.565	6.268	15.033	15.278

WWB	3.719	5.398	8.398	13.678
W1	5.080	5.324	13.849	14.310
W2	4.895	10.298	11.459	23.586

Cellulose based analysis regarding TGA and DTG

The thermal degradation of wood-based insulation materials within this inert atmosphere is restricted by the proportions of constituent main components of hemicellulose, cellulose and lignin [50]. The degradation of this material is a three-step process. Due to the wide variation in species and that the 'waste wood' may include different species of wood, the inherent differences between them the quantity and time taken for different mass loss of different samples will vary.

For cellulose based samples, initial mass loss can be attributed to evaporation within the fibre from the hydration adsorption of both intra and intermolecular reactions [51-53]. Extraction of water (by evaporation) can be demonstrated in cellulose samples up to 160°C [54]. However, after this cellulose degradation occurs at approximately 185°C [55] and as temperatures reach approximately 220°C the total degradation of cellulose begins. This degradation of the cellulose marks to beginning of the degradation of the two step thermal degradation pathway of the fibre[56]. As temperatures increase, hemicellulose continues to degrade and further exposure to temperatures at approximately 360°C begins the full degradation and charring of cellulose [57, 58]. It is evident from the figures 3a to 3h (below) that the degradation of these materials often overlap and occur in similar places.

Table 1 demonstrates that SMR and WP, shows no significant differences between the temperatures at which water evaporates within the sample. However, there is a difference between STW and WWB for water evaporation at 100°C and 300°C. Samples have a larger weight loss when stabilised at 53% by comparison to those at 75%. This demonstrates that for these materials, a differing hygrothermal environment alters their thermal properties. When comparing the amount of weight lost, STW at 75% has the largest initial mass loss (in addition to both samples of WWB). This shows their initial highly hygric properties, affecting the mass loss of WWB samples but not as significantly as 75% STW. From these 4 samples, SMR and WP are the most thermally stable are those which have not altered, despite the dynamic hygrothermal environment .

DTG was also used to understand the thermal stability of the cellulose based samples and samples experience three different steps: dehydration, active and pass pyrolysis [59]. As previously mentioned, the degradation of these materials initially is absorbed water (dehydration), the second stage of peaks correspond to cellulose and hemicellulose (active pyrolysis). Hemicellulose is usually a smaller 'shoulder peak' to the cellulose 'main peak' [54]. When lignin degrades, it exhibits (simultaneously) both active and passive pyrolysis over such a wide range of temperatures. Therefore it is extremely difficult to attribute what process is being observed for the curve within the curve [58]. The differences in temperature due to the different species of wood is outlined in [60] but is evidently a clear factor when considering the DTG curves in the following figures. For SMR, figures 3a (RH 53%) and 3b (RH 75%) demonstrates that from 200-250°C when stabilised at 75%, the

derivative peak is much more elongated and occurs over a shorter temperature range. By comparison to SMR at 53% this range is much larger and broadened demonstrating the results that in a differing hygrothermal environment there is a physico-chemical change in SMR which will directly affect its hygrothermal ability. Understanding this offers fundamental knowledge for the mechanisms that affect these materials moisture buffering capability within an indoor environment.

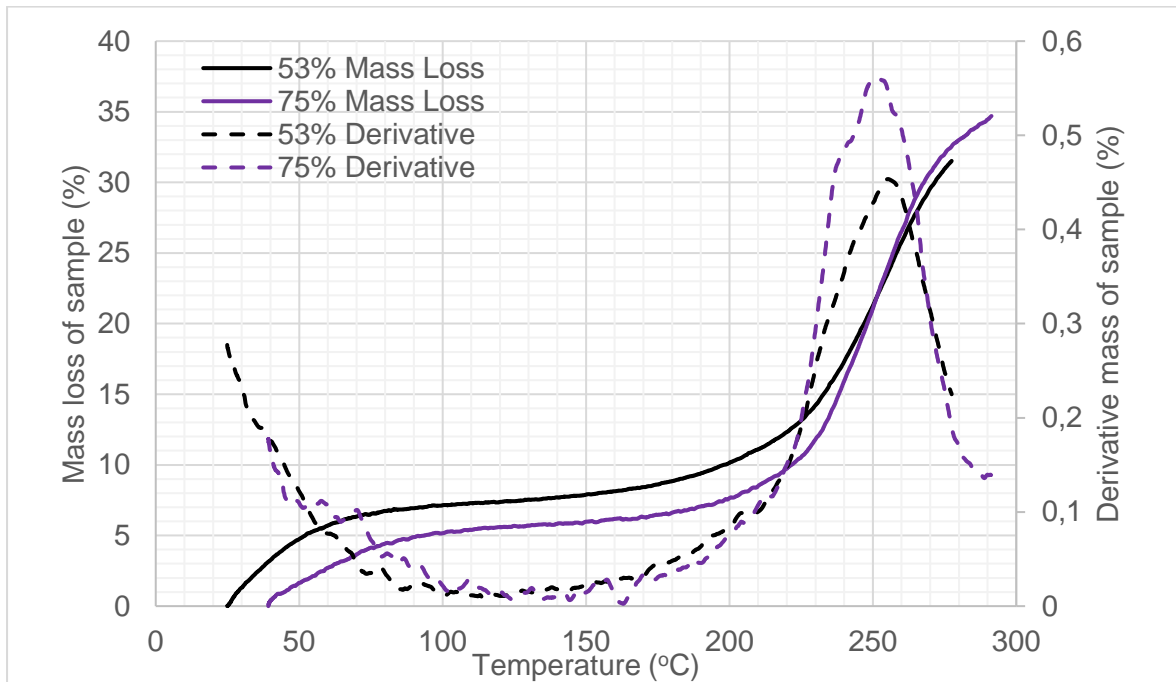


Figure 3a. TGA and DTG for SMR at 53% and 75%.

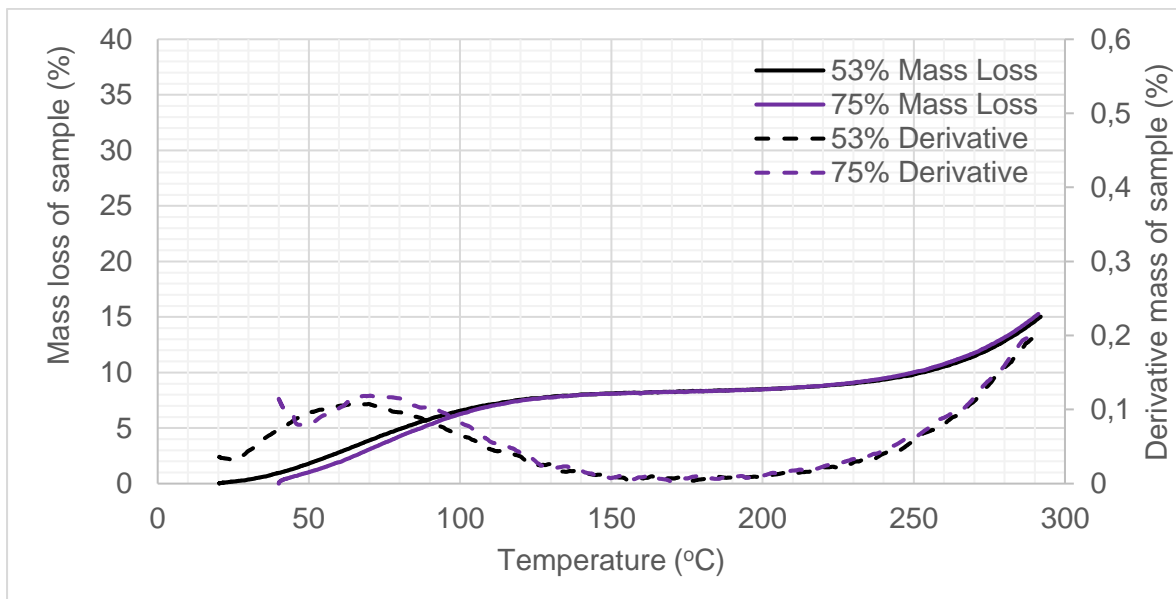


Figure 3b. TGA and DTG for WP at 53% and 75%.

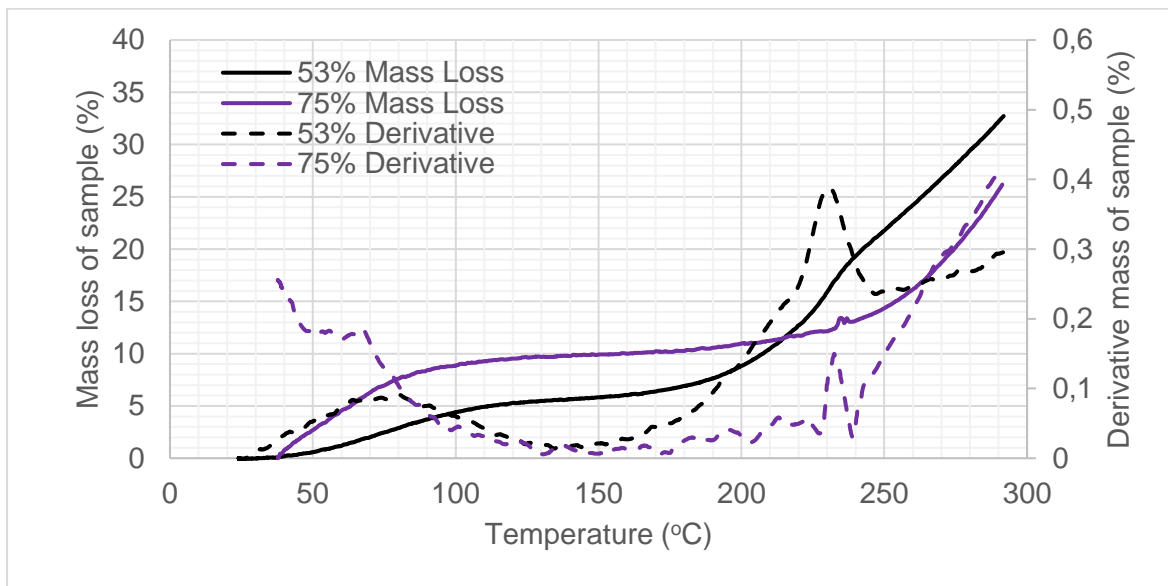


Figure 3c. TGA and DTG for STW at 53% and 75%.

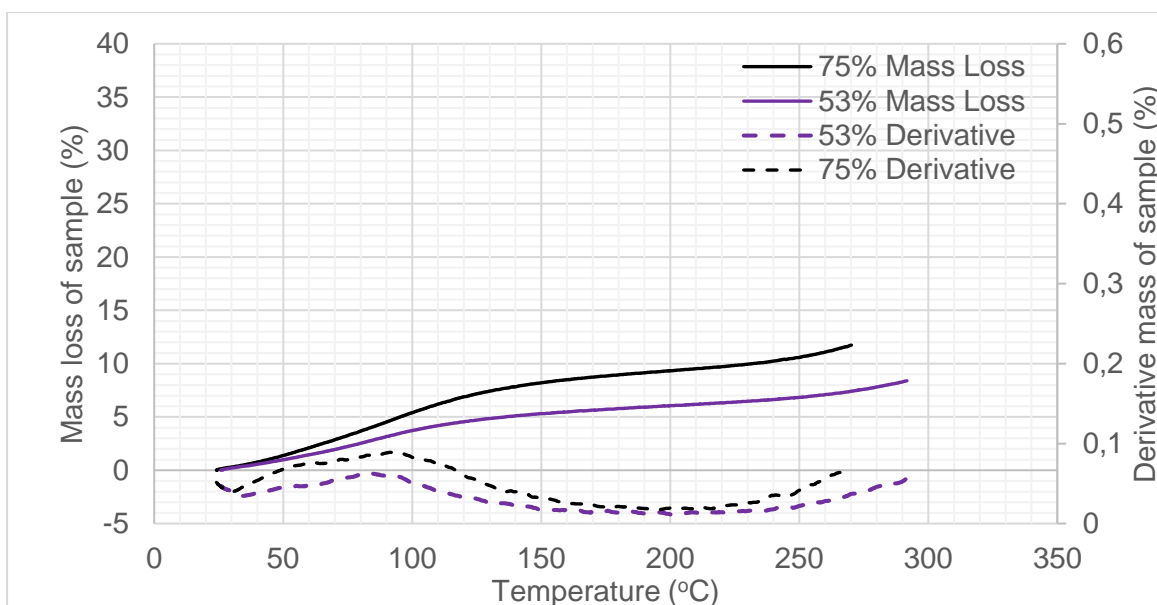


Figure 3d. TGA and DTG for WWB at 53% and 75%.

Keratin based analysis regarding TGA and DTG

TGA and DTG for W1 and W2 at 53% and 75% are demonstrated within figures 3e and 3f. Research for the thermogravimetric analysis of wool mainly comes from the textile industry where it has been examined that the melting point of wool decreases with increasing moisture content [12, 61] - outlined by Flory's theory [62]. This is when wool encounters water molecules and interacts with the polypeptides when crystallites melt. Another factor affecting melting point is the stability of structures,

the more stable the structure the higher the melting temperature as it can resist a greater amount of thermal degradation [63].

Initial mass losses within sample W1 are overall lower than that of W2 and the derivative of W1 at both RH's are similar. However, there is a greater increase in mass loss within 53% than 75% RH. By comparison, W2 has a larger peak for 75% at approximately 100°C associated to the moisture release within each sample. Water within samples takes 3 different forms: chemically bound water, loosely bound water and free water. Within a TGA curve these different types of water and the way in which it leaves the sample overlaps making it difficult to precisely identify [27]. The actual thermal and chemical degradation of wool molecules occurs at approximately 200°C [64]. So, when comparing weight loss after the release of water (within table 1) within the sample (before the chemical depletion of the molecule), it demonstrates that W1 has lost the least amount of mass therefore demonstrating its thermal stability. Therefore, it could be stated that due to the strong inner cross-linkages that the macromolecules have, W1 is less sensitive to a dynamic hygrothermal environment by comparison to W2 as outlined by concepts in [30, 32].

Although this method is useful for investigating the behaviour of these materials, it is not a “finger print” technique and can only indicatively mark the ‘typical’ behaviours in order to identify a sample therefore FTIR will be utilised in conjunction with TGA [65].

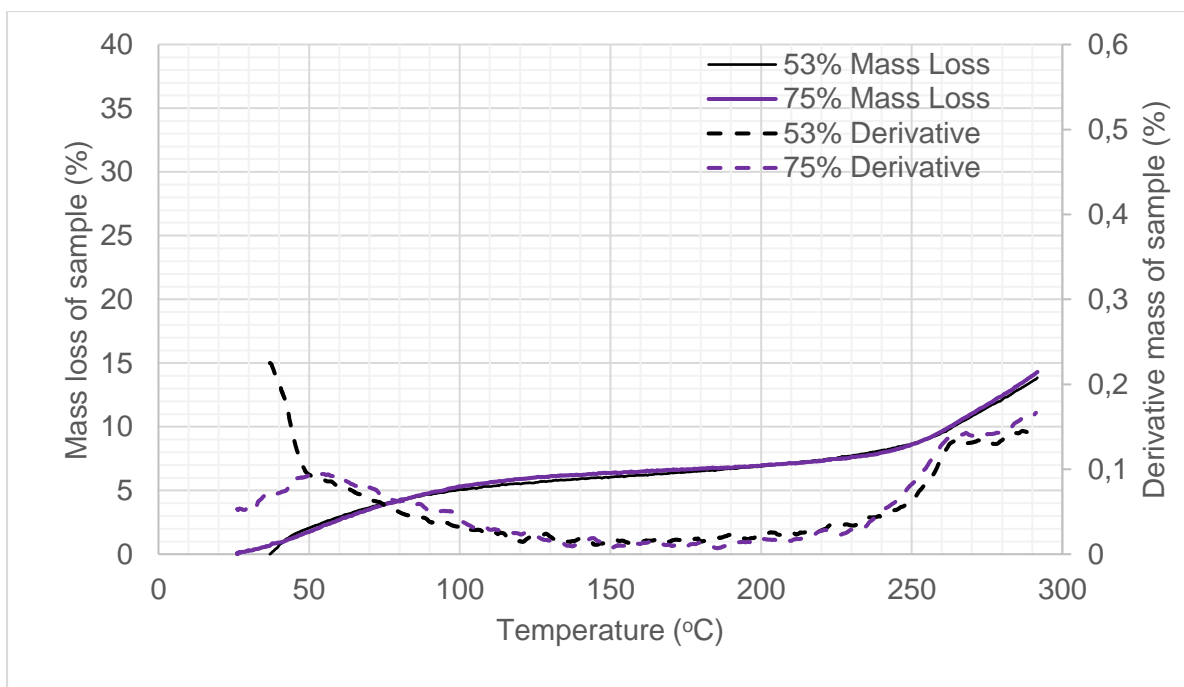


Figure 3e. TGA and DTG for W1 at 53% and 75%.

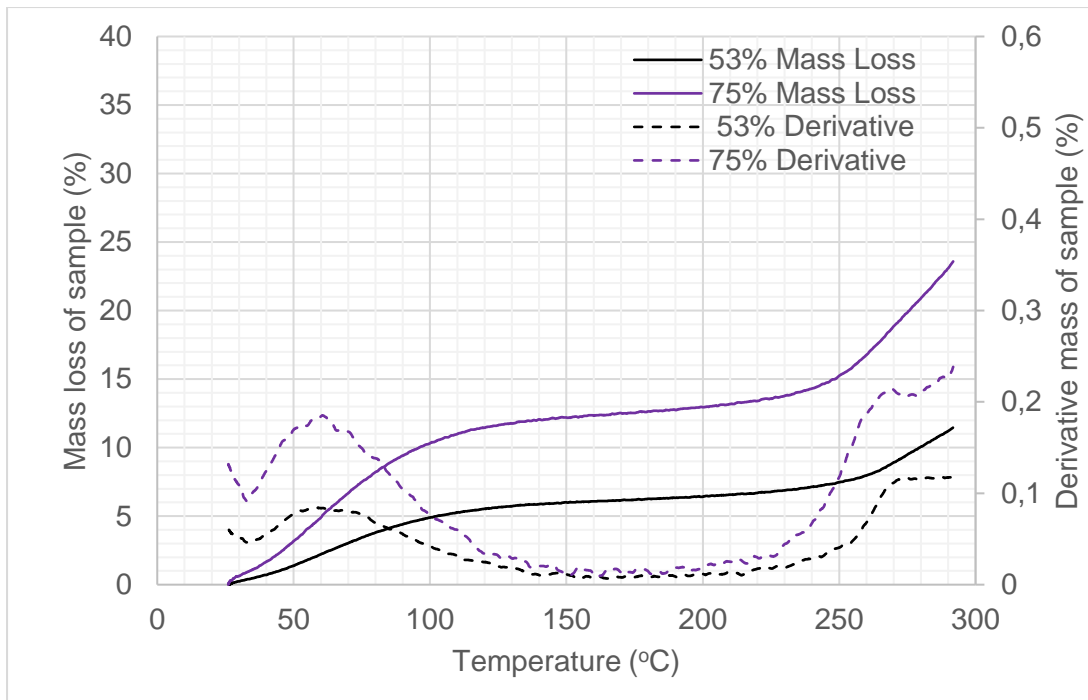


Figure 3f. TGA and DTG for W2 at 53% and 75%.

4.2 DSC

Utilising DSC will be utilised as a single step diagnostic tool for identifying and analysing patterns within phase transitions and understanding information about components within a samples[66]. Key thermal events that a DSC curve can map are: the evaporation of water, denaturation and glass transition[67]. This demonstrates that a physical transition or chemical reaction is taking place within the sample, the shape of the DSC curve is critical for deciphering the characteristics of the sample. The DSC thermograms for cellulose and keratin based samples will be analysed separately.

Cellulose Based analysis with DSC

The DSC thermograms for plant derived, cellulose based samples are demonstrated in figures 4a to 4d. The temperatures for key phase changes to the samples can be found within table 2. In cellulose based fibres (STW, WP, WWB, SMR) (with the exception of hydrogen bonding which are required for breaking and rebonding), there are no cross-linkages between molecules [68]. Between 25°C and 100°C, these hydrogen bonds are broken which give a greater range of freedom but less stillness and elasticity for the cellulose within the macromolecule[69].

Table 2. DSC phase transition temperatures for cellulose based samples.

Sample	Water Evaporation	Denaturation Temperature (T_d)
--------	-------------------	------------------------------------

		Temperature (T_{eva})	
SMR	53%	131.34	239.27
	75%	131.73	260.47
STW	53%	89.40	-
	75%	97.47	-
WP	53%	131.34	-
	75%	110.34	-
WWB	53%	126.47	-
	75%	133.47	-

From the literature, it is evident for all samples that an endothermic peak demonstrates the release of adsorbed water at approximately 100°C [52]. This is due to the vaporisation of water that is both within the sample's fibres and the interstitial spaces [70]. When comparing the evaporation temperatures of the different cellulose based samples (from table 3), it is evident that there is a wide difference in the way that water is released from the sample. STW has a lower evaporation temperature than the 'wooden based' samples SMR and WP. On the outer layer of STW have epidermal cells, these create a thin 'waxy' layer on the surface of the STW, making water vapour penetration difficult [71].

In terms of denaturation temperatures, for SMR there is a shift in the gradient of the heat flow, this step demonstrates an endothermic peak at 239.27°C for 53% and 260.47°C for 75% stabilised sample. This difference is substantial enough in order to suggest that there is a change within the SMR molecule when stabilised at differing RH. It is evident from table 2 that within this research paper, the DSC was run to 300°C and for STW and WP this temperature is not sufficient for denaturation to occur, implying that they are thermally the most stable out of all cellulose based samples. At further elevated temperatures, (approximately 330-360°C) cellulose based samples experience the degradation, dehydration and therefore the depolymerisation of cellulose [51, 72] leading it to char [27].

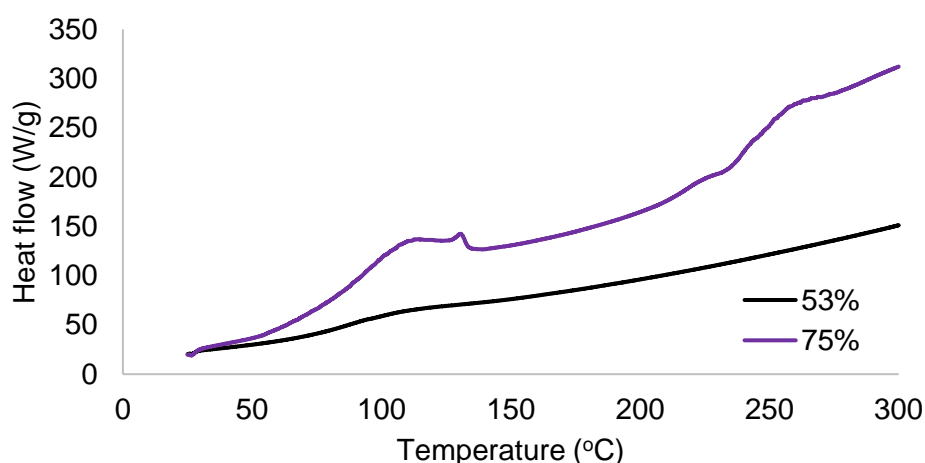


Figure 4a. SMR DSC thermogram.

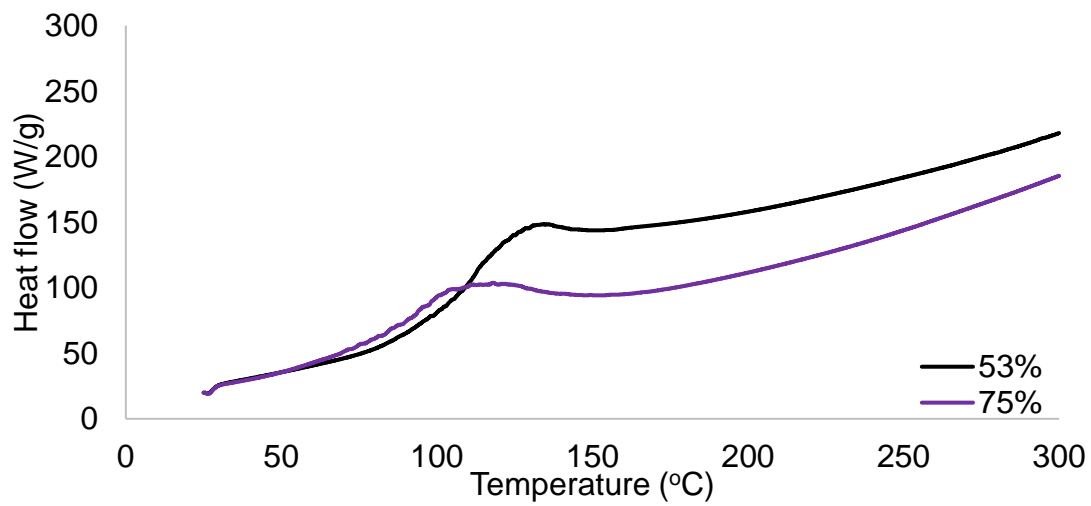


Figure 4b. WP DSC thermogram.

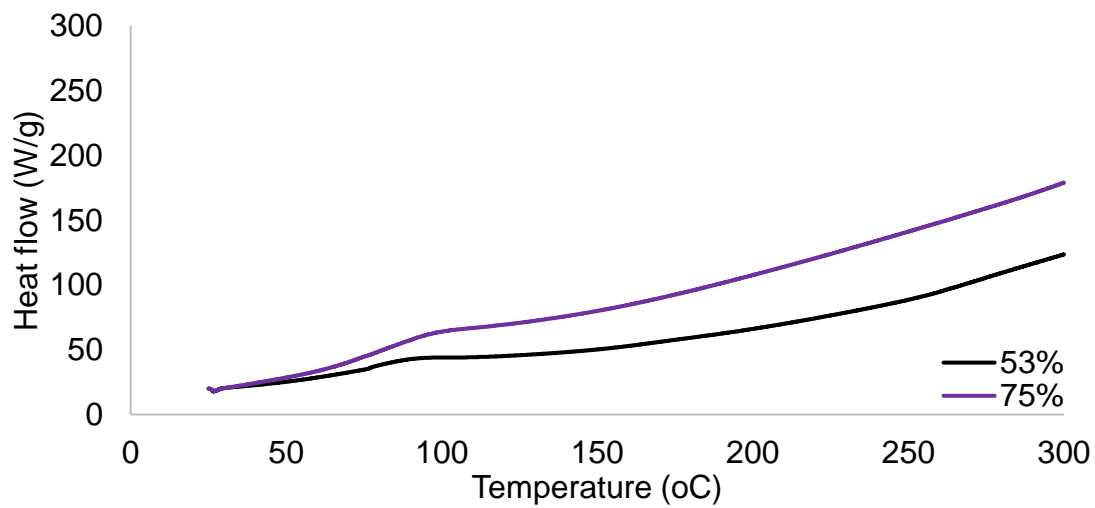


Figure 4c. STW DSC thermogram.

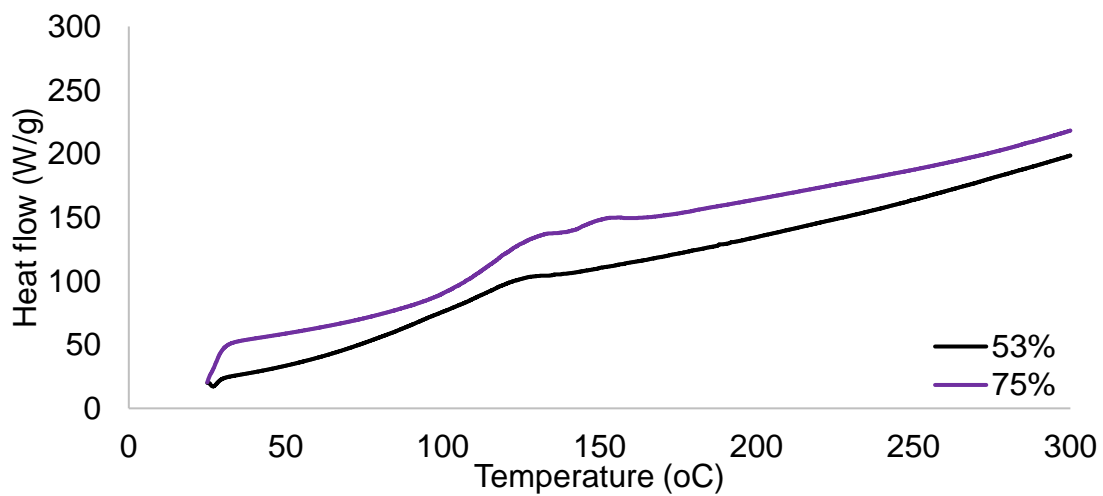


Figure 4d. WWB DSC thermogram.

Keratin Based analysis with DSC

For keratin-based materials, their thermograms are shown within Figures 4e and 4f. Key information for the different phases that the samples experienced are provided in Table 3. Glass transition is the first noted characteristic of this curve is between 40-60°C but overlaps with the initial water evaporation within the sample and therefore is difficult to analyse. Further to this, as a second order transition, glass transition occurs due to a relaxation of chain sections located within the amorphous part of the polymer [40]. Due to the fibrous nature of the wool, it can be difficult to accurately measure glass transition via DSC [73] in comparison with cellulose based samples which were discussed earlier. .

Table 3. DSC phase transition temperatures for keratin based samples.

Sample		Water Evaporation Temperature (T_{eva}) (°C)	Denaturation Temperature (T_d) (°C)
Wool 1	53%	124.60	256.94
	75%	89.60	253.60
Wool 2	53%	121.53	256.27
	75%	107.87	256.00

Following the glass transition, the water evaporation temperature (T_{eva}) occurs and due to the relationship between the water content of the fibres and water evaporation enthalpy this is an important link to the effect that relative humidity has on these samples. The denaturation temperature (T_d) is the temperature at which materials lose their quaternary, tertiary and secondary structure.

More broadly, thermal analysis within table 3 demonstrates that from approximately 25-100°C there is no degradation in the molecular chain due to there being no clear thermal events. As previously described water bonded to the fibre will evaporate from 30-150°C [69]. Table 3 shows that the water denaturation temperature is lower when samples are stabilised at higher RH's. It could be suggested that samples stabilised at a higher RH are less sensitive to temperature changes as the cross linkages within the inner macromolecules are stronger. When considering W1 and W2, as the evaporation temperature increases (T_{eva}) the interaction between the specific fibre and water molecules are stronger. When the wool based fibres adsorb more moisture, the interactions become more consistent and stronger.

Within Figure 4e and 4f it is evident that there is a secondary, small abrupt endotherm at approximately 250°C. This can be associated to the inner α -crystal within the wool molecule spilling and decomposing [61, 74]. Once the α -crystal has decomposed, if temperatures continue to rise further decomposition of β -keratin structure would be demonstrated [75].

Denaturation of the sample can be exhibited within the samples at approximately 250°C [73, 76]. Despite the difference in RH both W1 and W2 have very similar denaturation temperatures, suggesting that the RH has no effect on this property of the material. This could indicate that keratin based samples do not experience a change permanent chemical characteristics when stabilised at different RH). After the denaturation temperature, the different components of the wool sample are

decomposing [77]. Although this experimentation was from 25°C to 300°C, the literature explains how further increased temperatures would have exhibited the thermal breakage of intermolecular bonds and main chain degradation of the wool macromolecule [78] and further structural degradation up to 600°C.

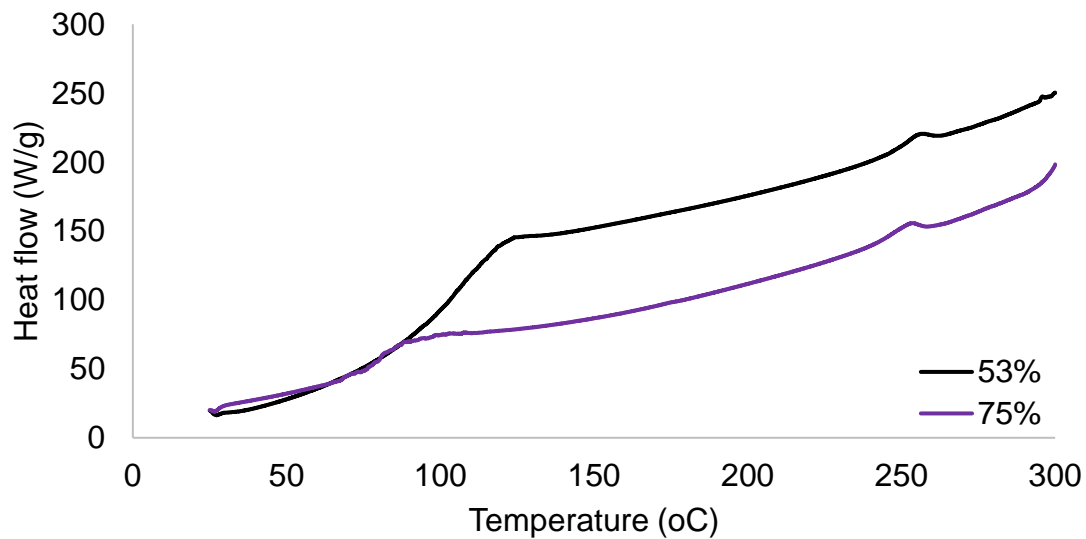


Figure 4e. Wool 1 DSC thermogram.

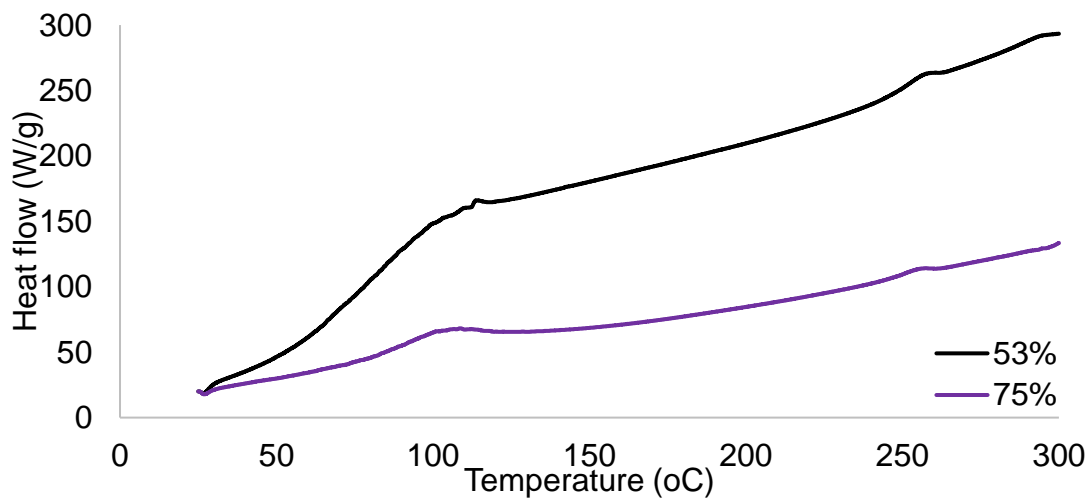


Figure 4f. Wool 2 DSC thermogram.

4.3 FTIR

This investigational technique enables to examine the molecular structure of the materials and to determine the chemical compositions via the demonstration of specific bonds as peaks or bands within a spectra. Within this experimentation, it will mainly focus on the functional group region of each spectra.

Cellulose Based analysis with FTIR

The 4 different cellulose based samples spectra can be found in Figures 5a to 5d. Within their core structure, all the bio-based materials within this research paper have hydroxyl groups which hydrogen bond with water in order to exhibit their hygrothermal characteristics. The fundamental mechanisms behind the way in which they do this has not been fully researched however, the assignment of bonds for each of the cellulose based samples can be found in table 5.

As highlighted in [79] FTIR highlights the ability of materials to adsorb water as a measure of the absorption of hydroxyl groups. Both inter- and intra- hydrogen bonds formed within the cellulose to water of each bio-fibre has demonstrated big differences on hydroxyl reactivity solubility and physical properties as outlined by [80]. All samples exhibit OH- stretching vibrations and sample have a larger adsorption band when stabilised at 75% by comparison to those at 53% [81]. The broadening of hydroxyl groups is due to the inter and intra hydrogen bonding taking place within the molecule [82]. The hydrogen bond network in cellulose is observed by [83] and despite the transmittance being relatively low, a weak 'hump' at approximately 1640cm^{-1} indicates carbon to carbon vibrations. However, as indicated by [60], this is masked by water adsorption at the same frequency. At this point for all cellulose based insulation materials, the hydroxyl groups are stretching and at higher relative humidity, this gain in water molecules increases the length of cellulose molecules and reduces intermolecular hydrogen bonding. Due to the location of these (-OH) groups within the cellulose their affinity to water is high.

When comparing all four samples to one another, there is a whole spectral difference in all samples which demonstrates how the spectra is affected by a difference in relative humidity and therefore water within the sample. For the cellulosic materials, there is a broadened absorption peak around 3000cm^{-1} when the materials are conditioned at a higher relative humidity. This adsorption peak can be associated to the inter and intramolecular hydrogen bonding as well as free/bound water within the material and free hydroxyls within the cellulose of the macromolecule.

By comparing figures 5a to 5d there are different sections of the spectra that are greatly affected by relative humidity by comparison to others. SMR, WP and STW all experience differences in adsorption intensities between $2935\text{-}2900\text{cm}^{-1}$ assigned to the CH bond stretching which is in line with [84] and demonstrates that this bond is affected by a differentiation in local hygrothermal environment.

In addition to this, from the works completed by [85], this work further supports that water molecules may coexist within each sample within both adsorption and desorption. Water exists in samples as 'free' and 'bound' water where free and bound water is exhibited at around 3000cm^{-1} whilst free water is exclusively found at approximately 1630cm^{-1} . These molecules bind to not only hydroxyl sites but also carboxyl function and the free water can diffuse into the porous bio-based fibres.

For SMR the transmittance is quite low and there are no major, strong bands within the material. However, there is a clear differentiation between the two different RH's for the same sample. Similarly to SMR, WP demonstrates that it is very affected in the hydroxyl region and this band is now much greater at 75% than 53% stabilisation. STW and WWB show that whilst the hydroxyl groups are affected the rest of the molecule is not as affected by its hygrothermal conditions in the same way that SMR and WP are. Table 4 demonstrates, Total Crystallinity (TCI), Intensity of

Hydrogen Bonding (HBI) and Lateral Order Index (LOI) for the 4 cellulose-based samples.

Table 4. TCI, HBI and LOI for 4 cellulose based samples.

Sample	TCI						HBI						LOI					
	I1370		I2900		I1370/I2900		I3400		I1320		I3400/I1320		I1430		I898		I1430/I898	
	53%	75%	53%	75%	53%	75%	53%	75%	53%	75%	53%	75%	53%	75%	53%	75%	53%	75%
SMR	92.09	86.83	90.64	85.18	1.02	1.02	94.02	85.63	92.27	87.13	1.02	0.98	91.50	85.06	88.23	82.09	1.04	1.04
WP	92.96	89.87	94.85	92.15	0.98	0.98	93.62	87.83	92.98	90.25	1.01	0.97	93.64	90.81	90.17	86.07	1.04	1.06
WWB	91.55	79.12	99.17	97.56	0.92	0.81	98.03	95.67	95.67	89.17	1.02	1.07	89.94	77.20	97.07	91.75	0.93	0.84
STW	74.96	77.76	79.28	81.65	0.95	0.95	80.88	76.94	77.50	79.24	1.04	0.97	79.04	81.28	67.24	65.78	1.18	1.24

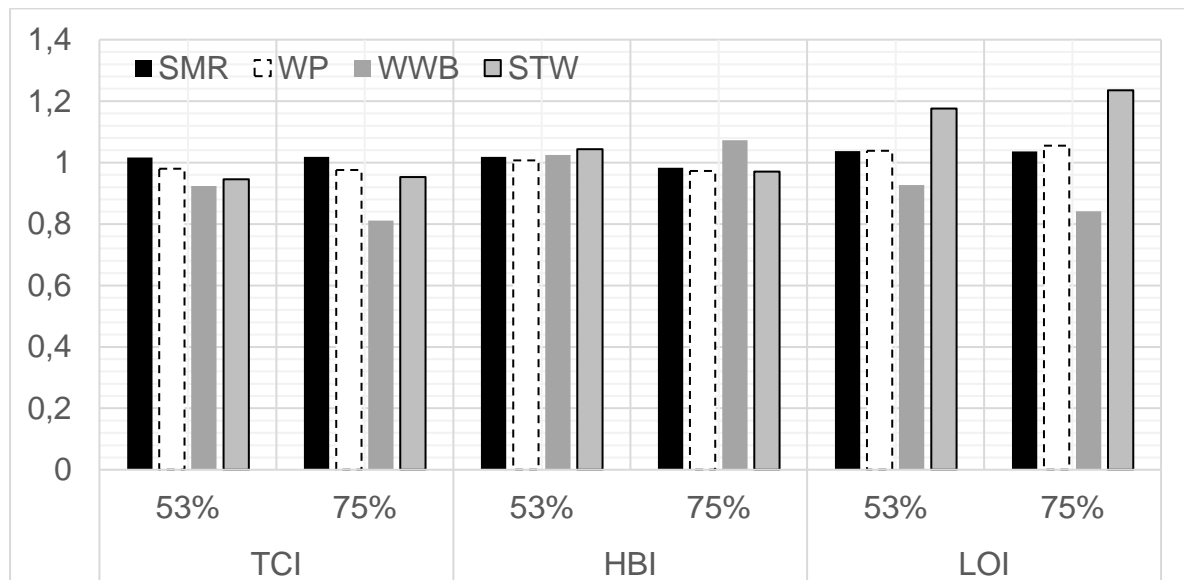


Figure 5. Total Crystallinity Index (TCI), Intensity of hydrogen bonding (HBI) and Lateral Order Index (LOI) for cellulose based samples.

When comparing the results from table 4 and Figure 5, SMR has the highest TCI at both RH (1.016 for 53% and 1.019 for 75% RH) by comparison to the WWB with the lowest (0.923 for 53% and 0.811 for 75%). However, as TCI decreases HBI increases and for all samples except for WWB, at 75% RH reduces the HBI. At 53% RH it is notable that all bio-based insulation samples have extremely similar HBI values. The LOI is particularly high in STW at both RH suggesting the molecule has a larger variation of the crystal lattice. [35] suggests that the thermal stability of samples which are cellulose based are affected by the order of the crystalline. Therefore, from Figure 5 it can be suggested that due to having the largest total crystallinity index, SMR is the most thermally stable bio-insulation sample.

Table 5. FTIR analysis of cellulose based samples and associated assignment of bonds at 53% and 75% RH.

SMR position of band (cm ⁻¹)		WP position of band (cm ⁻¹)		STW position of band (cm ⁻¹)		WWB position of band (cm ⁻¹)		Assignment for bond
53%	75%	53%	75%	53%	75%	53%	75%	
3270.739	3272.603	3335.967	3335.967	3280.057	3276.33	3408.65	3410.514	(OH) stretching vibration due to intermolecular hydrogen bonded and free groups [86-89] and stretching vibration of cellulose and lignin of the fibre [90] [91]
2912.915	2914.778			2847.686	2849.55			CH symmetrical stretching due to hemicellulose and cellulose components [92]
		2920.369	2920.369	2916.642	2918.506			Stretching vibrations of V(C=O) ester of cellulose and hemicellulose [93] and free hydroxyl group [94]
						1401.479	1399.615	C-O bond elongation of hemicellulose and cellulose [95-97]
1025.018	1025.018	1021.291	1023.154	1021.291	1026.882	872.1971	872.1971	(-CH-) bending vibration in cellulose [83]
				987.7445	987.7445			

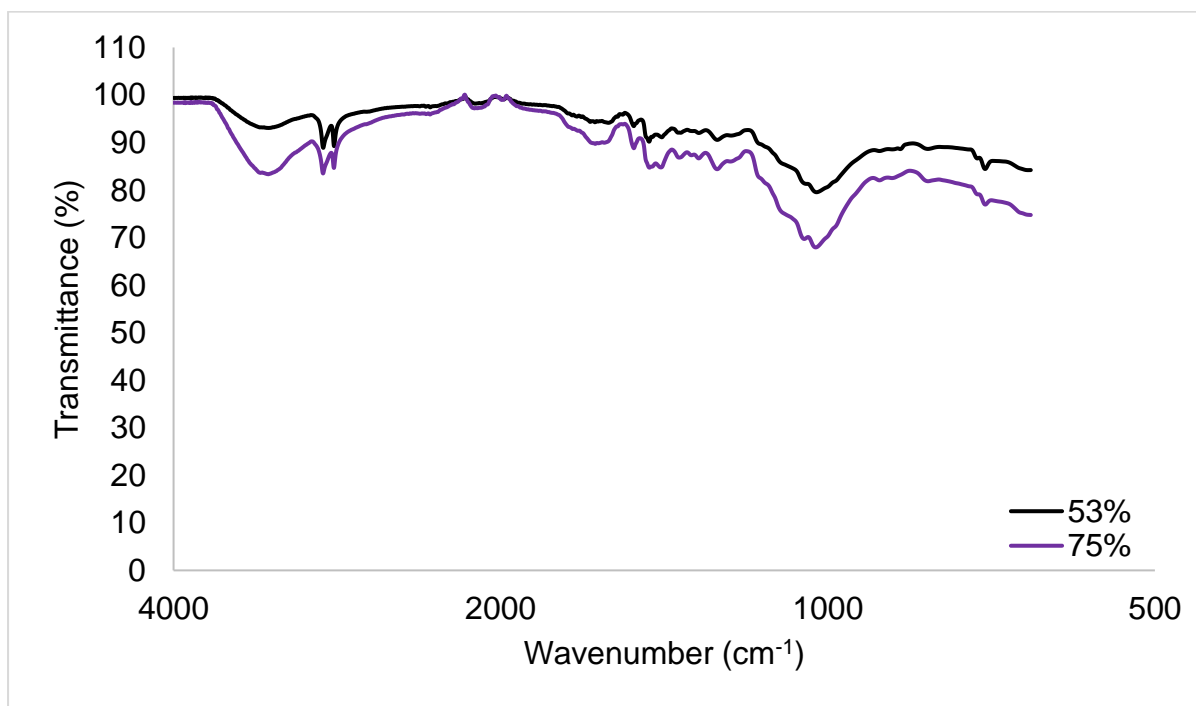


Figure 5a. SMR FTIR spectra.

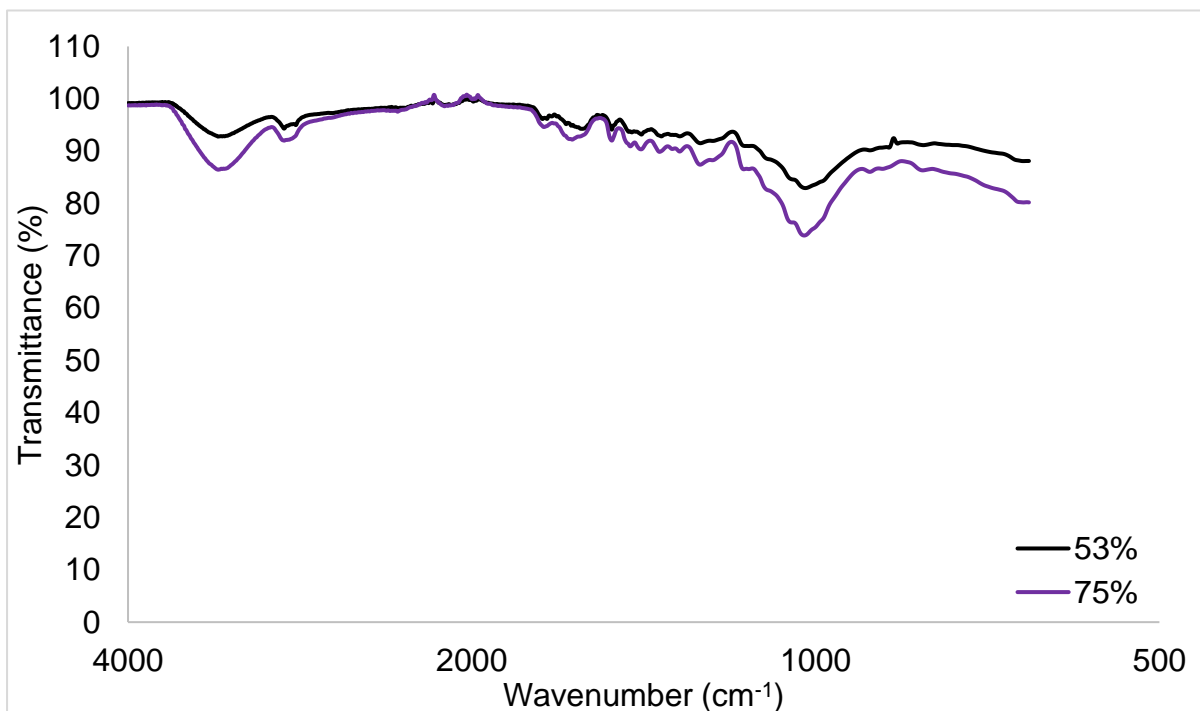


Figure 5b. WP FTIR spectra.

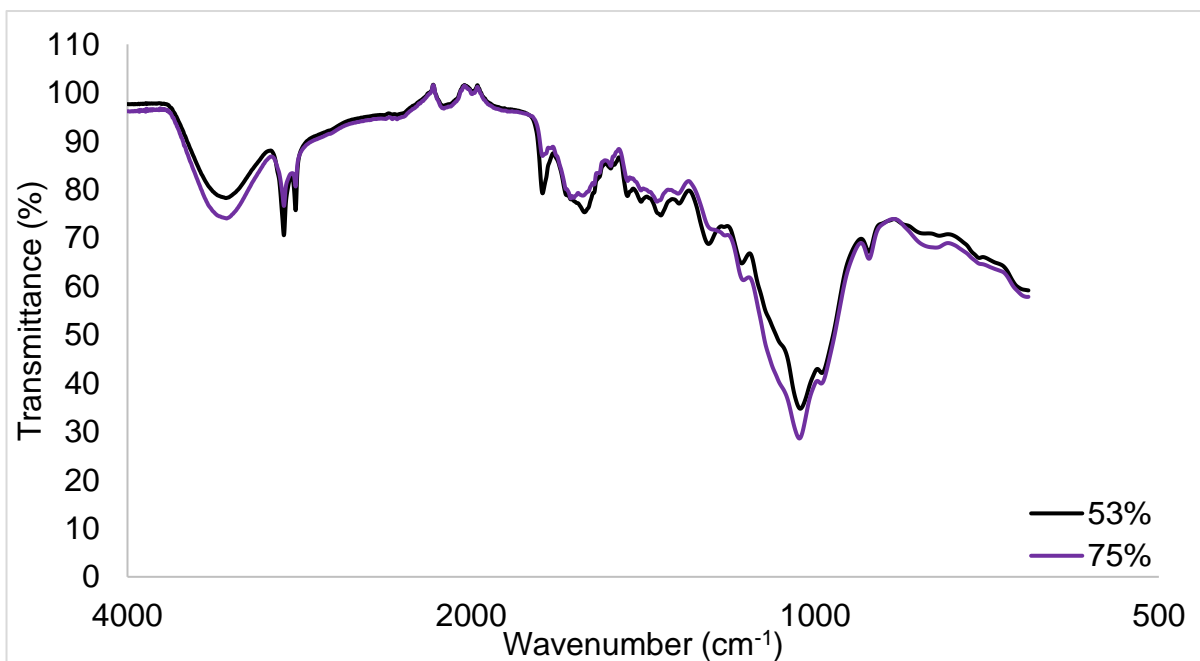


Figure 5c. STW FTIR spectra.

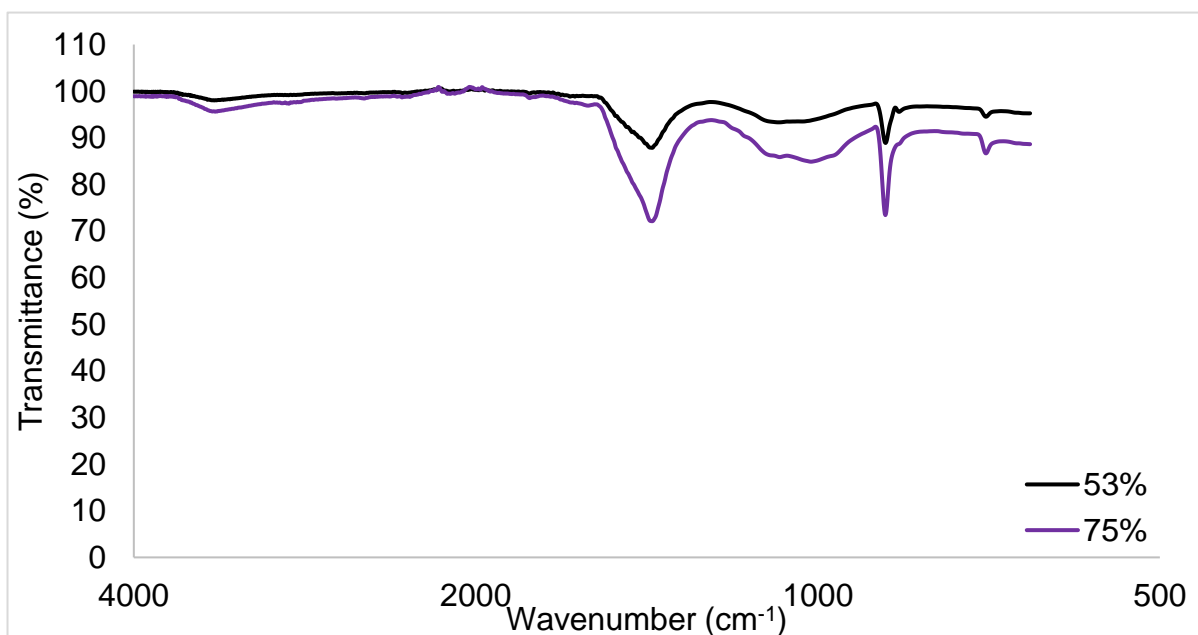


Figure 5d. WWB FTIR spectra.

Keratin Based analysis with FTIR

The spectra for WL1 and WL2 can be found in figures 5e and 5f (respectively) and assignment of bonds is demonstrated within Table 6. Within FTIR, the main characteristic bands appear between 1000 and 1700 cm^{-1} including: Amide I and Amide II [92, 98]. Amide I and Amide 2 are characteristic within the wool protein and the shape of this band is associated to the quantity and nature of hydrogen bonds within the molecule. Bands around 2900 and 1400 cm^{-1} represent CH_2 bonds and 2800 cm^{-1} is due to CH bonds [92] but due to Amide II forms a stretching vibration of $\text{C}=\text{O}$ at approximately 1620-40 cm^{-1} [99].

Due to inter and intra-hydrogen bonding, when placed in differing hygrothermal environments the hydroxyl group will fluctuate so becomes imperative to measure. The nature of these hydrogen bonds that are occurring will give a variety in the quantity and strength that the intermolecular interactions have. This varies greatly within the samples and causes the hydroxyl band to be broad (by comparison), when intermolecular reactions are weaker and therefore there is 'less' of a chemical environment for reactions to take place, bands are smaller and narrower. A bigger peak intensity from one sample to another (with the same peak position) demonstrates that there is more quantity of that specific type of bond. Any shifting or movement of the peak demonstrates an interaction has occurred. Further to this, if the band shape has changed (e.g. has broadened) displays interactions have occurred which is generally attributed to hydrogen bonding. For samples stabilised at 75%, their OH- absorption peak becomes bigger and broader indicating water gain, reducing the restraints of the hydroxyl group movement [69]. This is examined within W1 much more evidently than in W2 where in W1 the band has increased by comparison to the sample stabilised at 53%.

Table 6. FTIR analysis of keratin-based samples and associated assignment of bonds at 53% and 75% RH.

W1 position of band (cm ⁻¹)		W2 position of band (cm ⁻¹)		Assignment of Bond
53%	75%	53%	75%	
3265.148	3276.33	3263.284	3274.466	Presence of hydroxyl groups (-OH)
1626.983	1626.983	1636.301	1634.438	Stretching vibrations of C=O (Amide I) [100] [101]
1507.708	1507.708	1524.481	1522.618	Bending deformation peak of C-N-H (Amide II) [102]
1237.376	1239.34	1222.567	1239.34	Carbonyl oxygen C-O [102]

Regularity of the molecular chain (ROM) within these molecules can be calculated by utilising the intensity of the band at 1240cm⁻¹ and 1450cm⁻¹ [63]. These results are displayed in Table 7. The lower the ROM value is, the more disorder there is within the molecule [103]. W1 and W2 generally have very similar ROM values, however W2 generally has a lower value and is only slightly affected by the differing hygrothermal environment. By comparison, W1 is initially more ordered than W2 but after being conditioned at 75% becomes more disordered.

Table 7. ROM of keratin based molecules at 53% and 75%.

Sample ID	I1240		I 1450		I1240/ I 1450	
	53%	75%	53%	75%	53%	75%
W1	80.84	82.56	86.54	90.01	0.93	0.92
W2	84.27	81.40	91.71	88.68	0.92	0.92

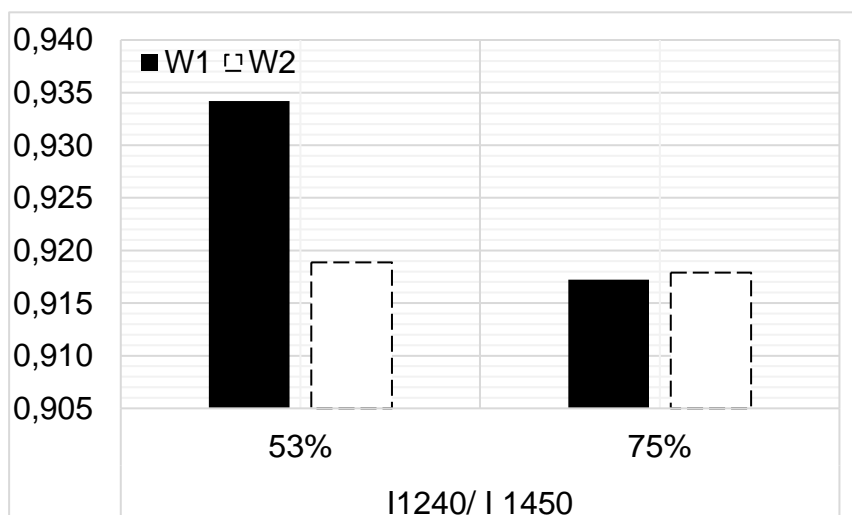


Figure 5e. Regularity of the molecular chain (ROM) for keratin-based samples.

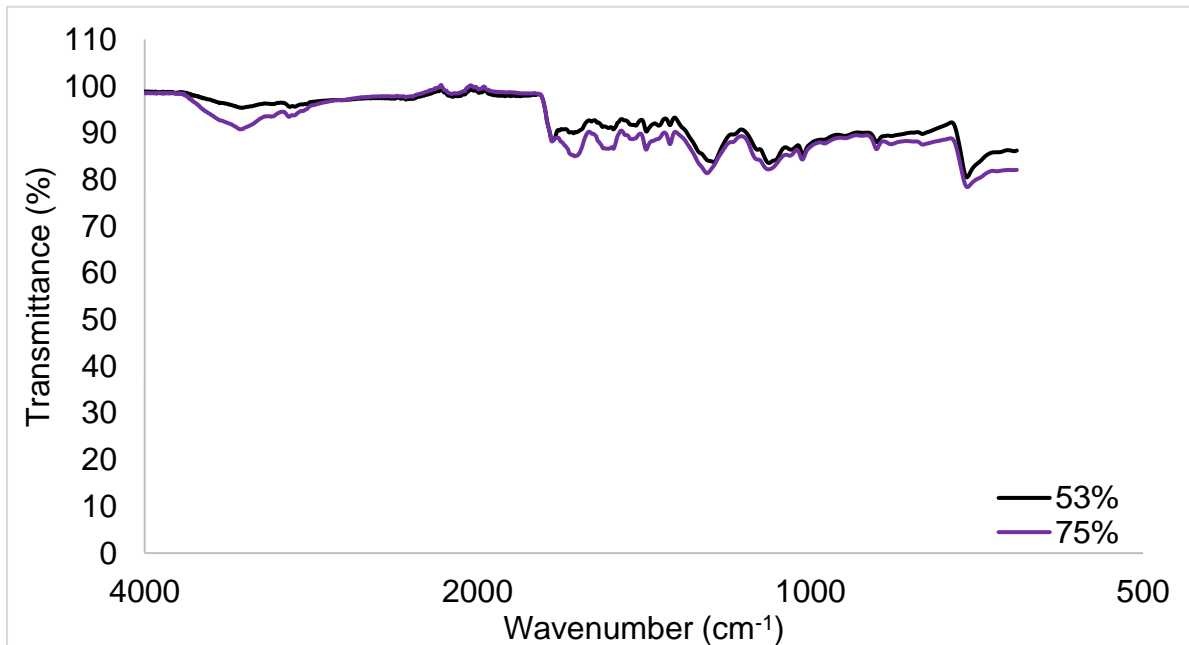


Figure 5e. W1 FTIR spectra.

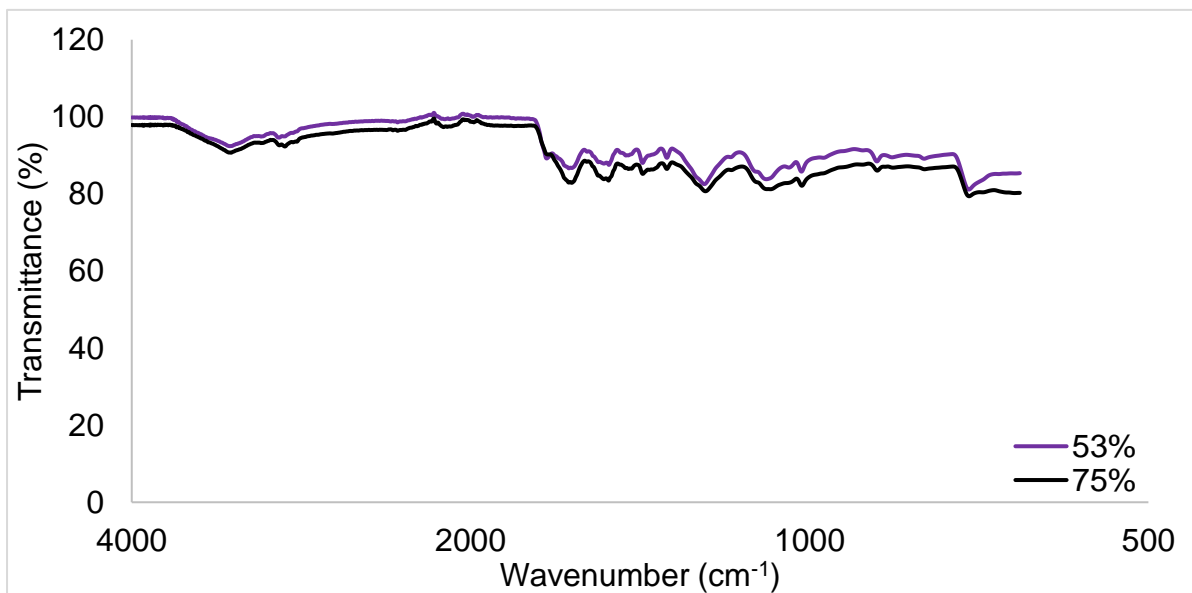


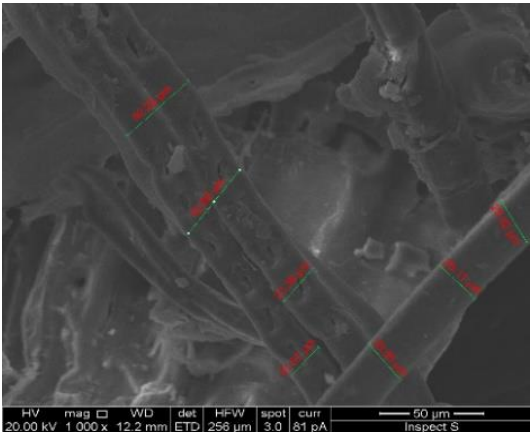
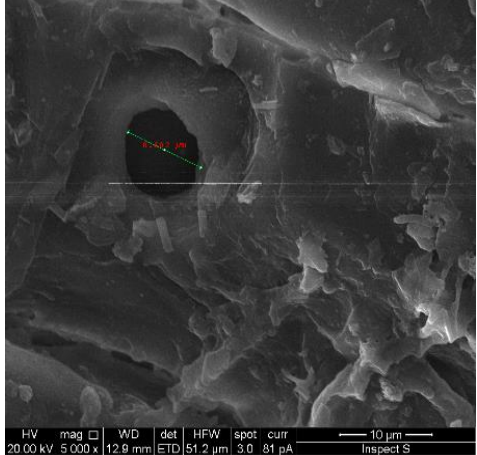
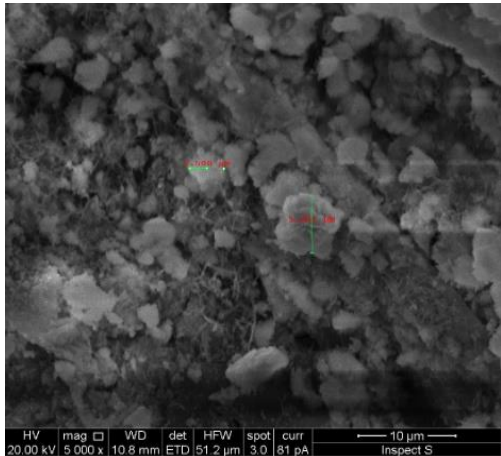
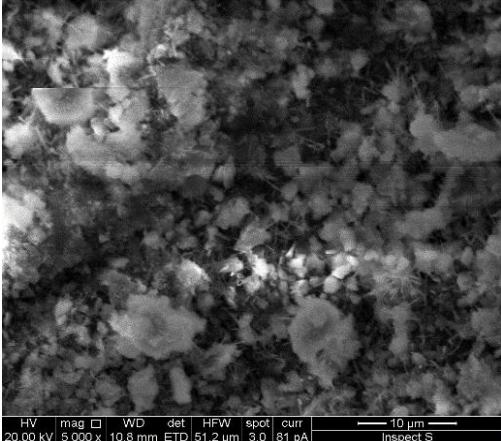
Figure 5f. W2 FTIR spectra.

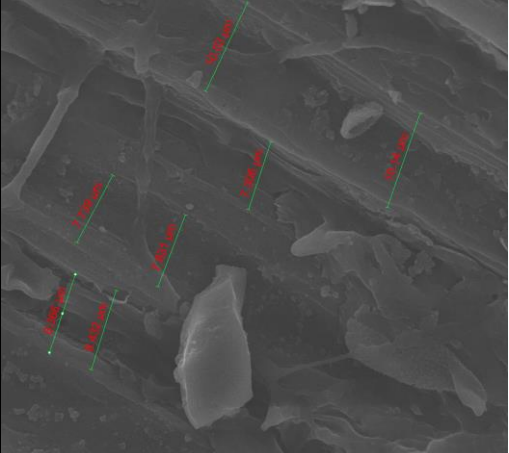
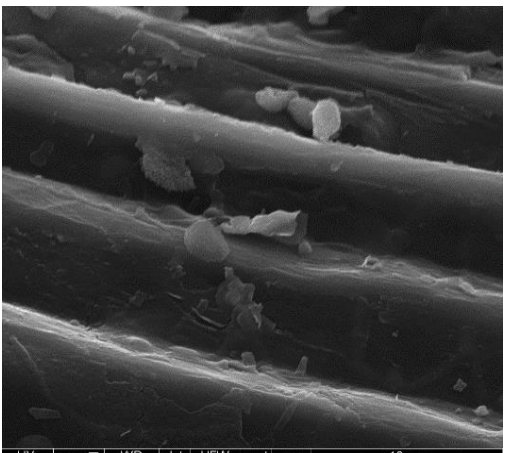
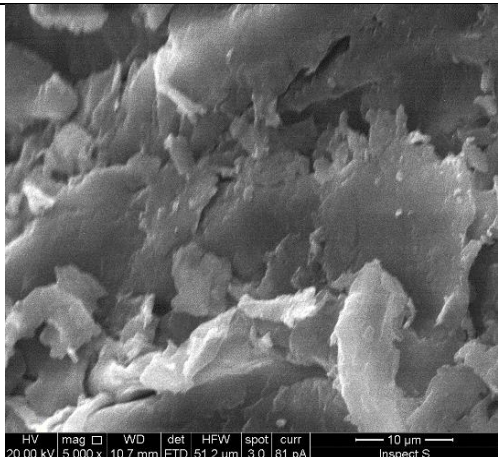
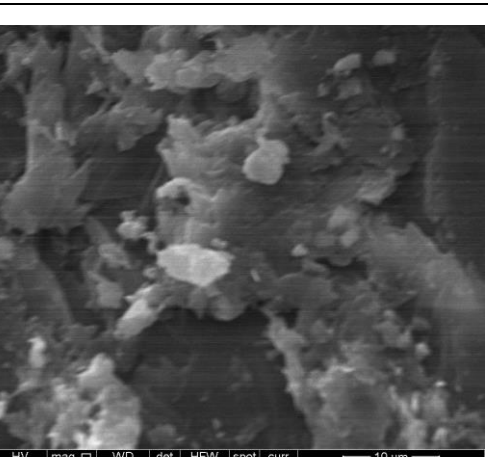
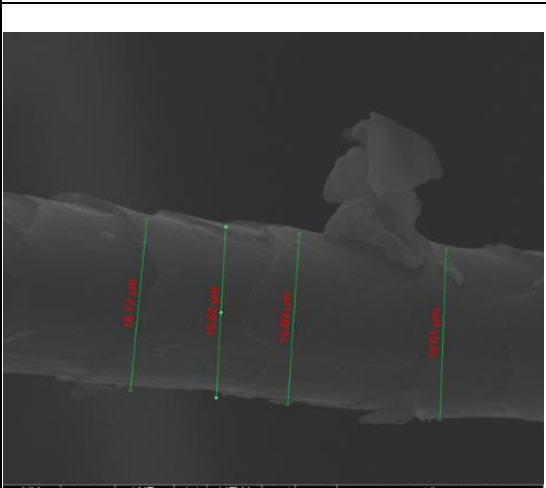
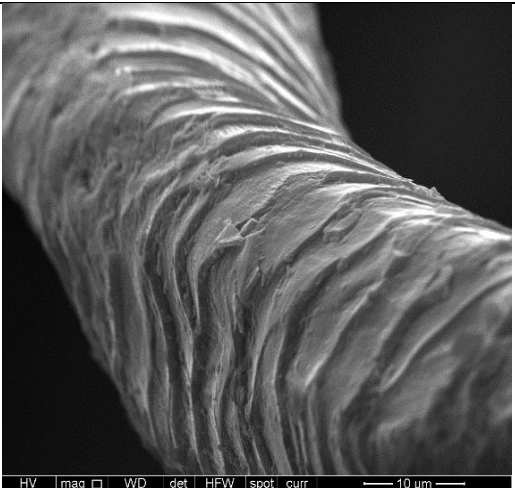
4.4 SEM

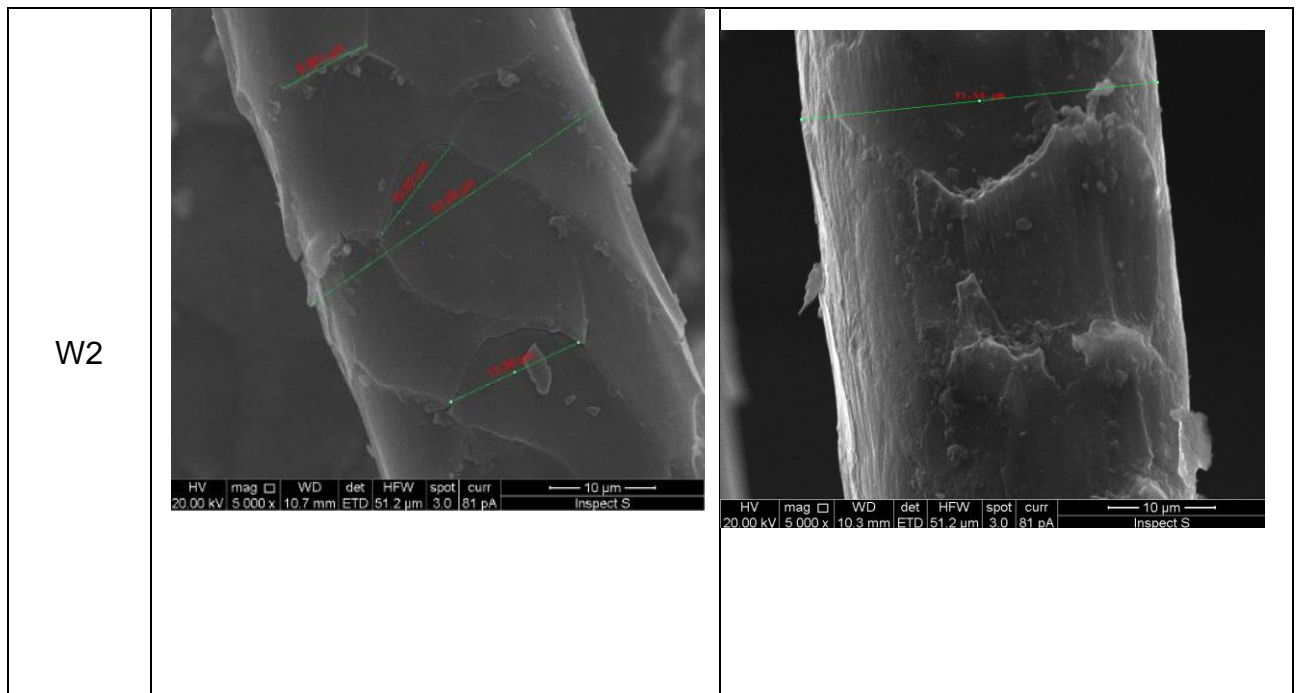
Providing three-dimensional, high resolution imagery of samples, SEM is important as it allows the user to understand morphological, topographical and physical properties of the samples. Table 8 demonstrates all insulation materials stabilised at 53% and 75%. When considering Table 8, it is evident that all samples have a complex surface morphology. For W1 and W2 it is evident from [104]] that the individual strands of fibre demonstrate even size and scale length. . When

considering the each strands surface texture, wool has an irregular, 'naturally crimped' surface morphology [105]. This fibrous morphology and irregular pattern on multiple planes by which these fibres interwind with each other makes this material suitable for good adhesion within a matrix (i.e. a mortar or grout). When considering SMR, WP, WWB and STW there is no clear and obvious optical differentiation between those stabilised at 53% and 75%.

Table 8. SEM Images of samples stabilised at 53% and 75% taken at 1000 and magnification.

Sample ID	53%	75%
SMR		
WWB		

<p>STW</p>	 <p>HV mag □ WD det HFW spot curr 20.00 kV 4.772 x 12.2 mm ETD 53.6 µm 3.0 81 pA 20 µm Inspect S</p>	 <p>HV mag □ WD det HFW spot curr 20.00 kV 5.000 x 12.1 mm ETD 51.2 µm 3.0 81 pA 10 µm Inspect S</p>
<p>WP</p>	 <p>HV mag □ WD det HFW spot curr 20.00 kV 5.000 x 10.7 mm ETD 51.2 µm 3.0 81 pA 10 µm Inspect S</p>	 <p>HV mag □ WD det HFW spot curr 20.00 kV 5.000 x 13.7 mm ETD 51.2 µm 3.0 81 pA 10 µm Inspect S</p>
<p>W1</p>	 <p>HV mag □ WD det HFW spot curr 20.00 kV 5.000 x 11.5 mm ETD 51.2 µm 3.0 81 pA 10 µm Inspect S</p>	 <p>HV mag □ WD det HFW spot curr 20.00 kV 5.000 x 10.0 mm ETD 51.2 µm 3.0 81 pA 10 µm Inspect S</p>



5. Conclusion

This paper has demonstrated multiple different thermochemical methods in order to detect differences between 6 different bio-based insulation samples, stabilised at 53% and 75%. Consisting of two fundamentally differing structures the samples were split into cellulose (SMR, STW, WWB, and WP) and keratin (W1 and W2) based materials.

- Using TGA, it was demonstrated that in a dynamic hygrothermal environment SMR and WP are the most hygrothermally stable and for keratin-based materials W1 is the most stable.
- DSC demonstrated that whilst STW and WP did not reach their denaturation temperature within this experimentation SMR and WWB temperature remained the same, despite their different stabilisation RH. Whereas wool based materials demonstrated little differentiation between the two samples.
- In terms of FTIR for cellulose based materials, when comparing spectra and absorbance's at different frequencies shows the overall crystallinity index. This indicates that SMR has the highest thermal stability for cellulose based samples. For the keratin-based samples when conditioned at 75%, W2 has the more ordered structure but W1 is affected more in terms of hydroxyl absorbance from the spectra.
- When comparing using SEM to compare samples, despite having a greater understanding of their surface morphology, there are not significant and obvious differences between samples conditioned at different RH.

It is evident from this experimentation that the differences between bio-based samples conditioned at different RH fundamentally affects their physical properties and interactions but is difficult to generally quantify due to their heterogeneous nature. Overall, in terms of cellulose based materials, SMR has

demonstrated that it is the most thermally stable and due to being little differentiation between the samples except for in TGA – W1 demonstrates the most thermally stable characteristics.

Acknowledgments

The author would like to thank lab technician Rob Allen in the School of Pharmacy and Biomolecular Sciences at LJMU.

References

1. Burke, M.J. and J.C. Stephens, *Political power and renewable energy futures: A critical review*. Energy Research & Social Science, 2018. **35**: p. 78-93.
2. Liu, L., et al., *The development history and prospects of biomass-based insulation materials for buildings*. Renewable and Sustainable Energy Reviews, 2017. **69**: p. 912-932.
3. Pérez-Lombard, L., J. Ortiz, and C. Pout, *A review on buildings energy consumption information*. Energy and Buildings, 2008. **40**(3): p. 394-398.
4. Jones, D. and C. Brischke, *Performance of Bio-based Building Materials*. 2017: Elsevier Science.
5. Jerman, M. and R. Černý, *Effect of moisture content on heat and moisture transport and storage properties of thermal insulation materials*. Energy and Buildings, 2012. **53**: p. 39-46.
6. Romano, A., et al., *On the development of self-controlled bio-based panels for building's thermal management*, in *European Conference on Composite Materials 2018*: Athens, Greece.
7. Joshi, S.V., et al., *Are natural fiber composites environmentally superior to glass fiber reinforced composites?* Composites Part A: Applied Science and Manufacturing, 2004. **35**(3): p. 371-376.
8. McDonough, W., *Cradle to cradle : remaking the way we make things*, ed. M. Braungart. 2002, New York: New York : North Point Press.
9. Palumbo, M., J. Formosa, and A.M. Lacasta, *Thermal degradation and fire behaviour of thermal insulation materials based on food crop by-products*. Construction and Building Materials, 2015. **79**(Supplement C): p. 34-39.
10. Zheng, C., D. Li, and M. Ek, *Mechanism and kinetics of thermal degradation of insulating materials developed from cellulose fiber and fire retardants*. Journal of Thermal Analysis and Calorimetry, 2019. **135**(6): p. 3015-3027.
11. Gur'ev, V. and S. Khainer, *Correlation of structure and thermal conductivity of highly disperse porous-fiber materials under variations of temperature and moisture*. Glass and Ceramics, 1999. **56**(11-12): p. 364-368.
12. Romano, A., et al., *Dynamic behaviour of bio-based and recycled materials for indoor environmental comfort*. Construction and Building Materials, 2019. **211**: p. 730-743.
13. Karamanos, A., S. Hاديarakou, and A.M. Papadopoulos, *The impact of temperature and moisture on the thermal performance of stone wool*. Energy and Buildings, 2008. **40**(8): p. 1402-1411.

14. D'Alessandro, F., et al., *Experimental assessment of the water content influence on thermo-acoustic performance of building insulation materials*. Construction and Building Materials, 2018. **158**: p. 264-274.
15. Troppová, E., et al., *Influence of temperature and moisture content on the thermal conductivity of wood-based fibreboards*. Materials and Structures, 2015. **48**(12): p. 4077-4083.
16. Holcroft, N. and A. Shea, *Moisture buffering and latent heat effects in natural fibre insulation materials*. 2013.
17. Jorgensen, W.L. and J.D. Madura, *Temperature and size dependence for Monte Carlo simulations of TIP4P water*. Molecular Physics, 1985. **56**(6): p. 1381-1392.
18. Rawat, S.P.S. and D.P. Khali, *Studies on adsorption behaviour of water vapour in lignin using the Brunauer-Emmett-Teller theory*. Holz als Roh- und Werkstoff, 1999. **57**(3): p. 203-204.
19. Straube, J.F., *Moisture and materials*. Building Science Digest, 2006. **138**: p. 1-7.
20. Céline, A., et al., *Characterization and modeling of the moisture diffusion behavior of natural fibers*. Journal of Applied Polymer Science, 2013. **130**(1): p. 297-306.
21. Feist, M., *Thermal analysis: basics, applications, and benefit*. ChemTexts, 2015. **1**(1): p. 8.
22. Frost, R.L. and A.M. Vassallo, *The Dehydroxylation of the Kaolinite Clay Minerals using Infrared Emission Spectroscopy*. Clays and Clay Minerals, 1996. **44**(5): p. 635-651.
23. Bernal, S., et al., *Characterization of supplementary cementitious materials by thermal analysis*. Materials and Structures, 2017. **50**(1): p. 1-13.
24. Tsujiyama, S. and A. Miyamori, *Assignment of DSC thermograms of wood and its components*. Thermochim. Acta, 2000. **351**(1-2): p. 177-181.
25. Ball, R., A. C. Mcintosh, and J. Brindley, *The role of char-forming processes in the thermal decomposition of cellulose*. Physical Chemistry Chemical Physics, 1999. **1**(21): p. 5035-5043.
26. Yorulmaz, S.Y. and A.T. Atimtay, *Investigation of combustion kinetics of treated and untreated waste wood samples with thermogravimetric analysis*. Fuel Processing Technology, 2009. **90**(7): p. 939-946.
27. Rahman, M., S. Hamdan, and J. Hui, *Differential Scanning Calorimetry (DSC) and Thermogravimetric Analysis (TGA) of Wood polymer nanocomposites*. MATEC Web of Conferences, 2017. **87**: p. 03013.
28. Tarrío-Saavedra, J., et al., *Functional nonparametric classification of wood species from thermal data*. Journal of Thermal Analysis and Calorimetry, 2011. **104**(1): p. 87-100.
29. Adl-Zarrabi, B., *Determination of Thermal Properties of Wood and Wood Based Products by Using Transient Plane Source*. 2004.
30. Cancellieri, V., D. Cancellieri, and E. Leoni, *Relation between forest fuels composition and energy emitted during their thermal degradation*. Journal of Thermal Analysis and Calorimetry, 2009. **96**: p. 293-300.
31. Yang, Y., et al., *Structural ATR-IR analysis of cellulose fibers prepared from a NaOH complex aqueous solution*. IOP Conference Series: Materials Science and Engineering, 2017. **213**: p. 012039.
32. Nelson, M.L. and R.T. O'Connor, *Relation of certain infrared bands to cellulose crystallinity and crystal latticed type. Part I. Spectra of lattice types I,*

- II, III and of amorphous cellulose*. Journal of applied polymer science, 1964. **8**(3): p. 1311-1324.
33. Poletto, M., et al., *Materials Produced From Plant Biomass. Part II: Evaluation of Crystallinity and Degradation Kinetics of Cellulose*. Materials Research, 2012. **15**: p. 421-427.
 34. Corgié, S.C., H.M. Smith, and L.P. Walker, *Enzymatic transformations of cellulose assessed by quantitative high-throughput fourier transform infrared spectroscopy (QHT-FTIR)*. Biotechnology and Bioengineering, 2011. **108**(7): p. 1509-1520.
 35. Cai, Y., et al., *Preparation, Morphology and Properties of Electrospun Lauric Acid/PET Form-Stable Phase Change Ultrafine Composite Fibres*. Polymers and Polymer Composites, 2011. **19**: p. 773-780.
 36. Temiz, A., et al., *Combustion properties of alder (Alnus glutinosa L.) Gaertn. subsp. barbata (C.A. Mey) Yalt.) and southern pine (Pinus sylvestris L.) wood treated with boron compounds*. Construction and Building Materials, 2008. **22**(11): p. 2165-2169.
 37. McGregor, B.A., X. Liu, and X.G. Wang, *Comparisons of the Fourier Transform Infrared Spectra of cashmere, guard hair, wool and other animal fibres*. The Journal of The Textile Institute, 2018. **109**(6): p. 813-822.
 38. Micheal, M.N. and N.A. El-Zaher, *Efficiency of ultraviolet/ozone treatments in the improvement of the dyeability and light fastness of wool*. Journal of Applied Polymer Science, 2003. **90**(13): p. 3668-3675.
 39. El-Amoudy, E.S. and E.M. Osman, *Thermal stability and fastness properties of wool fabric dyed with an ecofriendly natural dye "sambucus nigra" under the effect of different mordants*. Applied Chemistry, 2012. **44C**: p. 7080-7085.
 40. Osman, E. and N. Abd El-Zaher, *Effect of Mordant Type on Thermal Stability and Fastness Properties of Silk Fabric Dyed with Natural Dye "Sambucus Nigra"*. Vol. 15. 2011. 61-70.
 41. Gibson, P.W., *Effect of Wool Components in Pile Fabrics on Water Vapor Sorption, Heat Release and Humidity Buffering*. Journal of Engineered Fibers and Fabrics, 2011. **6**(1): p. 155892501100600102.
 42. Palumbo, M., *Contribution to the development of new bio-based thermal insulation materials made from vegetal pith and natural binders: hygrothermal performance, fire reaction and mould growth resistance*. 2015.
 43. Üreyen, M., et al., *Effect of polyamide ratio on the flammability of wool/PA blended aircraft seat fabrics*. IOP Conference Series: Materials Science and Engineering, 2018. **460**: p. 012033.
 44. Johnson, N.A.G., et al., *Wool as a Technical Fibre*. The Journal of The Textile Institute, 2003. **94**(3-4): p. 26-41.
 45. Forouharshad, M., et al., *Flame retardant wool using zirconium oxychloride in various acidic media optimized by RSM*. Thermochemica Acta, 2011. **516**(1-2): p. 29-34.
 46. Laborel-Préneron, A., et al., *Plant aggregates and fibers in earth construction materials: A review*. Construction and Building Materials, 2016. **111**(Supplement C): p. 719-734.
 47. Schiavoni, S., et al., *Insulation materials for the building sector: A review and comparative analysis*. Renewable and Sustainable Energy Reviews, 2016. **62**: p. 988-1011.

48. ISO, I.O.f.S., *BS EN ISO 12570:2000 Hygrothermal performance of building materials and products. Determination of moisture content by drying at elevated temperature*, in BSI. 2000.
49. Romano, A., et al. *BIO-BASED AND RECYCLED MATERIALS: CHARACTERISATION AND HYGROTHERMAL ASSESSMENT FOR PASSIVE RELATIVE HUMIDITY MANAGEMENT*. in *International Conference of Bio-based Building Materials (ICBBM)*. 2019. Belfast, UK.
50. Alén, R., E. Kuoppala, and P. Oesch, *Formation of the main degradation compound groups from wood and its components during pyrolysis*. *Journal of Analytical and Applied Pyrolysis*, 1996. **36**(2): p. 137-148.
51. Fairbridge, C. and R.A. Ross, *A kinetic and surface study of the thermal decomposition of cellulose powder in inert and oxidizing atmospheres*. *Journal of applied polymer science*, 1978. **22**(2): p. 497-510.
52. Martin, A., et al., *Studies on the thermal properties of sisal fiber and its constituents*. *Thermochimica Acta*, 2010. **506**: p. 14–19.
53. Liu, Z., et al., *Thermal Decomposition Characteristics of Chinese Fir*. *BioResources*, 2013. **8**(4): p. 5014-5024.
54. Gašparovič, L., Z. Koreňová, and Ľ. Jelemenský, *Kinetic study of wood chips decomposition by TGA*. *Chemical Papers*, 2010. **64**(2): p. 174-181.
55. Jabbar, A., et al., *Tensile, surface and thermal characterization of jute fibres after novel treatments*. *Indian J. Fibre Text. Tes.*, 2016. **41**(3): p. 249-254.
56. Alabdulkarem, A., et al., *Thermal analysis, microstructure and acoustic characteristics of some hybrid natural insulating materials*. *Construction and Building Materials*, 2018. **187**: p. 185-196.
57. Ali, M.E. and A. Alabdulkarem, *On thermal characteristics and microstructure of a new insulation material extracted from date palm trees surface fibers*. *Construction and Building Materials*, 2017. **138**: p. 276-284.
58. Haiping, Y., et al., *Characteristics of Hemicellulose, Cellulose and Lignin Pyrolysis*. *Fuel*, 2007. **86**: p. 1781-1788.
59. Fengel, D., *Wood chemistry, ultrastructure, reactions*, ed. G. Wegener. 1989, Berlin

New York: Berlin

New York : Walter de Gruyter.

60. González-Díaz, E. and J.-M. Alonso-López, *Characterization by thermogravimetric analysis of the wood used in Canary architectural heritage*. *Journal of Cultural Heritage*, 2017. **23**: p. 111-118.
61. Cao, J. and A. Bhojro, *Structural Characterization of Wool by Thermal Mechanical Analysis of Yarns*. *Textile Research Journal*, 2001. **71**: p. 63-66.
62. Cao, J., *DSC Studies of the Melting Behavior of α -Form Crystallites in Wool Keratin*. 1997. **v. 67**(no. 2): p. pp. 117-123-v.67 no.2.
63. Li, Q., C. Hurren, and X. Wang, *CHANGES IN WOOL PROTEIN STRUCTURE AND FABRIC PROPERTIES WITH ULTRASONIC TREATMENT*. 2019.
64. Price, D. and A.R. Horrocks, *1 - Combustion processes of textile fibres*, in *Handbook of Fire Resistant Textiles*, F.S. Kilinc, Editor. 2013, Woodhead Publishing. p. 3-25.
65. Haines, P., et al., *Principles of Thermal Analysis and Calorimetry*. 2002, Cambridge, UNITED KINGDOM: Royal Society of Chemistry.

66. Reh, U., G. Kraepelin, and I. Lamprecht, *Use of Differential Scanning Calorimetry for Structural Analysis of Fungally Degraded Wood*. Applied and Environmental Microbiology, 1986. **52**(5): p. 1101.
67. Martí, M., et al., *Thermal analysis of merino wool fibres without internal lipids*. Journal of Applied Polymer Science, 2007. **104**: p. 545-551.
68. Lewin, M., *Handbook of Fiber Chemistry*. Vol. 3rd Edition. 2006, Boca Raton: CRC Press.
69. Xia, Z., et al., *Comparative study of cotton, ramie and wool fiber bundles' thermal and dynamic mechanical thermal properties*. Textile Research Journal, 2016. **86**(8): p. 856-867.
70. Belaadi, A., et al., *Thermochemical and statistical mechanical properties of natural sisal fibres*. Composites Part B, 2014. **67**: p. 481-489.
71. Pizzi, A. and K.L. Mittal, *Wood Adhesives*. Vol. 1. 2011, London: CRC Press.
72. Shafizadeh, F. and G.W. Bradbury, *A kinetic model for pyrolysis of cellulose*. Journal of applied polymer science, 1979. **23**(11): p. 3271-3280.
73. Marti, M., et al., *Thermal analysis of merino wool fibres without internal lipids*. Journal of Applied Polymer Science, 2007. **104**(1): p. 545-551.
74. Hsieh, S.-H., et al., *Antimicrobial and physical properties of woolen fabrics cured with citric acid and chitosan*. Journal of Applied Polymer Science, 2004. **94**(5): p. 1999-2007.
75. Xu, W., et al., *Characterization of Superfine Wool Powder/Poly(propylene) Blend Film*. Macromolecular Materials and Engineering, 2007. **292**: p. 674-680.
76. Zargarkazemi, A., et al., *Modification of wool fabric using prepared chitosan/cyanuric chloride hybrid*. The Journal of The Textile Institute, 2014. **106**.
77. Cao, J., *Melting study of the α -form crystallites in human hair keratin by DSC1 Presented at the 9th Chinese Conference on Chemical Thermodynamics and Thermal Analysis (CTTA), Beijing, China, August 1998.1*. Thermochimica Acta, 1999. **335**(1): p. 5-9.
78. WI, X., *Thermal analysis of ultrafine wool powder*. 2003. **87**: p. 2372.
79. Maskell, D., et al., *PROPERTIES OF BIO-BASED INSULATION MATERIALS AND THEIR POTENTIAL IMPACT ON INDOOR AIR QUALITY*, in *First International Conference on Bio-based Building Materials*. 2015: Clermont-Ferrand, France.
80. Fan, M., D. Dai, and B. Huang, *3 Fourier Transform Infrared Spectroscopy for Natural Fibres*. Fourier Transform-Materials Analysis, 2012.
81. Maréchal, Y. and H. Chanzy, *The hydrogen bond network in I β cellulose as observed by infrared spectrometry*. Journal of Molecular Structure, 2000. **523**(1): p. 183-196.
82. Abdel-Kareem, O. and K. Elnagar, *Non-Destructive Methods to Investigate the Deterioration Extent of Coptic Egyptian Textiles*. 2005. **4**.
83. Garside, P. and P. Wyeth, *Identification of Cellulosic Fibres by FTIR Spectroscopy I: Thread and Single Fibre Analysis by Attenuated Total Reflectance*. Studies in Conservation, 2003. **48**.
84. Céline, A., et al., *Qualitative and quantitative assessment of water sorption in natural fibres using ATR-FTIR spectroscopy*. Carbohydrate Polymers, 2014. **101**: p. 163-170.

85. Carter, H.G. and K.G. Kibler, *Langmuir-Type Model for Anomalous Moisture Diffusion In Composite Resins*. Journal of Composite Materials, 1978. **12**(2): p. 118-131.
86. Owen, N.L. and D.W. Thomas, *Infrared Studies of "Hard" and "Soft" Woods*. Applied Spectroscopy, 1989. **43**(3): p. 451-455.
87. Hinterstoisser, B. and L. Salmén, *Two-dimensional step-scan FTIR: a tool to unravel the OH-valency-range of the spectrum of Cellulose I*. Cellulose, 1999. **6**(3): p. 251-263.
88. KONDO, T., *The assignment of IR absorption bands due to free hydroxyl groups in cellulose*. Cellulose, 1997. **4**(4): p. 281.
89. Dai, D. and M. Fan, *Characteristic and Performance of Elementary Hemp Fibre*. Materials Sciences and Applications, 2010. **01**: p. 336-342.
90. Brígida, A.I.S., et al., *Effect of chemical treatments on properties of green coconut fiber*. Carbohydrate Polymers, 2010. **79**(4): p. 832-838.
91. Schwanninger, M., et al., *Schwanninger M , Rodriguez JC , Pereira H , Hinterstoisser B . Effects of short-time vibratory ball milling on the shape of FT-IR spectra of wood and cellulose*. Vibr. Spec. Vibrational Spectroscopy, 2004. **36**: p. 23-40.
92. Wojciechowska, E., A. Włochowicz, and A. Weselucha-Birczyńska, *Application of Fourier-transform infrared and Raman spectroscopy to study degradation of the wool fiber keratin*. Journal of Molecular Structure, 1999. **511-512**: p. 307-318.
93. Morshed, M.M., M.M. Alam, and S.M. Daniels, *Plasma treatment of natural jute fibre by rie 80 plus plasma tool*. Plasma Science and Technology, 2010. **12**(3): p. 325-329.
94. Rana, R., et al., *FTIR spectroscopy, chemical and histochemical characterisation of wood and lignin of five tropical timber wood species of the family of Dipterocarpaceae*. Wood Science and Technology, 2010. **44**(2): p. 225-242.
95. El Hajam, M., et al., *Physicochemical characterization of softwood waste "Cedar" and hardwood waste "Mahogany": comparative study*. Materials Today: Proceedings, 2019. **13**: p. 803-811.
96. Hori, R. and J. Sugiyama, *A combined FT-IR microscopy and principal component analysis on softwood cell walls*. Carbohydrate Polymers, 2003. **52**(4): p. 449-453.
97. Popescu, C.M., et al., *Spectral characterization of eucalyptus wood*. Appl Spectrosc, 2007. **61**(11): p. 1168-77.
98. Church, J.S., G.L. Corino, and A.L. Woodhead, *The analysis of Merino wool cuticle and cortical cells by Fourier transform Raman spectroscopy*. Biopolymers, 1997. **42**(1): p. 7-17.
99. Vasconcelos, A., G. Freddi, and A. Cavaco-Paulo, *Biodegradable Materials Based on Silk Fibroin and Keratin*. Biomacromolecules, 2009. **10**: p. 1019.
100. Liu X., et al., *FTIR Spectrum and Dye Absorption of Cashmere and Native Fine Sheep Wool*, in *Proc. 4th Int. Cashmere Determination Techniques Symposium*. 2008: China.
101. Pelton, J.T. and L.R. McLean, *Spectroscopic methods for analysis of protein secondary structure*. Anal Biochem, 2000. **277**(2): p. 167-76.
102. Gallagher, W. *FTIR Analysis of Protein Structure, Chem 455, Biochemistry Lab II - Synthesis and Characterisation of Amyloid Fibril - Forming Peptides - Manuals*. in *Polymer International*. 2005.

103. Huson, M., J. Church, and G. Heintze, *Spectroscopy, microscopy and thermal analysis of the bi-modal melting of Merino wool*. Wool Technology and Sheep Breeding, 2001. **50**: p. 64-75.
104. Langley, K.D. and T.A. Kennedy, *The Identification of Specialty Fibers*. Textile Research Journal, 1981. **51**(11): p. 703-709.
105. Yao, P., et al., *Characterization of Secondary Structure Transformation of Stretched and Slenderized Wool Fibers with FTIR Spectra*. Journal of Engineered Fibers and Fabrics, 2008. **3**.